Successful Establishment of In-vivo Selective Liver Lobe Decellularization: The starting point for In-vivo Liver Engineering

Dissertation
in partial fulfilment of the requirements for the degree of doctor medicinae (Dr. med.)

submitted to the Faculty Council of the School of Medicine at Friedrich Schiller University of Jena

by An Wang
born on 05.03.1982 in Hainan

Gutachter:

1. **Prof. Dr. med. Uta Dahmen**

Experimentelle Transplantationschirurgie,

Klinik für Allgemein-, Viszeral- und Gefäßchirurgie, Universitätsklinikum Jena

2. **Herr PD Dr. med. habil. Gerd Fabian Volk**

Klinik für Hals-, Nasen- und Ohrenheilkunde,Oberarzt, Universitätsklinikum Jena

3. **Herr doc. MUDr. Václav Liška, Ph.D.**

Laboratory of Cancer Treatment and Tissue Regeneration

Faculty of Medicine in Pilsen Biomedical Center , Charles University

Datum der Verteidigung: 01.10.2019

Table of contents

Abbreviations

ECM: Extracellular matrix

PVDC: Polyvinylidene choloride

SDS: Sodium dodecyl sulfate

SEM: Scanning electronic microscopy

PV: Portal vein

CV: Central vein

Zusammenfassung

Hintergrund:

Biologisches "Organ engineering" ist ein neues Verfahren um protentiell transplantierbare Organe zu generieren. Dabei wird das Organ explantiert, dezellularisiert und anschließend repopuliert. Bisher wurden zahlreiche Protokolle zur Dezellularisierung etabliert. Aktuell gibt es weitaus weniger Kenntnisse zur erfolgreichen Repopulation und lediglich präliminäre Berichte zur Kurzzeitfunktion (maximal 72h) nach Transplantation einzelner repopulierter Leberlappen. Die Langzeitfunktion des transplantierten Lebergerüsts ist immer noch eine Zukunftsvision. Daher ist eine alternative zum Ex-vivo "Liver engineering" erforderlich um die Bedingungen der funktionellen Repopulierung besser zu verstehen.

Vor kurzem (2016) hat die Arbeitsgruppe von PAN über ihre Arbeiten zur In-vivo-Dezellularisierung und Repopulation des rechten unteren Lappens bei der Ratte berichtet. Alle Versuchstiere wurden jedoch nach 6 Stunden intraoperativer Beobachtungszeit getötet, da eine schwere Gewebeschädigung durch das Detergenz vermutet wurde.

Ziel:

Das Ziel dieser Studie ist die Entwicklung eines Überlebensmodells für die selektive in-vivo Dezellularisierung eines Leberlappens im Rattenmodell.

Methoden und Ergebnisse:

Im der **ersten Manuskript I (Jove 2018, IF 1.3)** haben wir unser neues chirurgisches Modell der selektiven Perfusion des links-lateralen Leberlappens bei der Ratte vorgestellt. Der gewählte Leberlappen wurde für entweder 20 min, 1h, 2h oder 4h (n=3/Gruppe) mit Heparin-Kochslazlösung gespült. Unabhängig von der Perfusionszeit wurde die Prozedure von allen tieren gut toleriert (Einwochenüberlebensrate von 100%, 12/12 Tieren). Histologisch fanden sich bereits nach 20min Perfusion keiebnrlie Blutzellen mehr im Gefäßsystem, Weder in der Portalven, noch in den Sinusoiden oder den Lebervenen.

Im **zweiten Manuskript II (eingereicht bei Acta Biomaterialia, IF 6.3)** haben wir drei verschiedene Protokolle verglichen, um das optimale Verfahren für die In-vivo-Dezellularisierung zu ermitteln. Wir beobachteten, dass bei zweistündiger Perfusion mit 1% SDS anstelle von 1% Triton X100 oder 1% Triton X100, gefolgt von 1% SDS die In-vivo-Dezellularisierung des gewählten Leberlappens in etwa 2 Stunden reproduzierbar zur histologisch vollständigen Entfernung aller Zellkomponenten führte.

Die so generierten Lebergerüste wurde weiter charakterisiert. Die Integrität der Gefäßstruktur einschließlich der Pfortader, der Leberarterie, des Gallengangs und der zentralen Vene sowie der Mikro- und Ultrastruktur der Matrix wurde durch CT, Histologie und SEM bestätigt. Wir konnten immunhistochemisch zeigen, daß die Hauptmatrixproteine, einschließlich Collagen I und IV, Elastin, Fibronectin und Laminin, erhalten blieben, und wir somit ein qualitativ hochwertigs Lebergerüst generierten.

Außerdem haben wir zwei Drainagemethoden verglichen, um die optimale Methode zur Organprotektion während der In-vivo-Dezellularisierung zu ermitteln. Mit Hilfe der kompletten Abdeckung der Organe mit einem Polyvinylidenchlorid-Film und Kompressen bei gleichzeitiger Platzierung eines Absaugkatheters konnten wir eine Einwochenüberlebensrate von 100% erreichen (n=6/6), im Gegensatz zu nur 16,7% (n =1/6) ohne Verwedung des Absaugkatheters.

Als letztes untersuchten wir die Interaktion zwischen Blut und dem Lebergerüst 12h nach Reperfusion. Zu diesem Zeitpunkt fanden sich histologisch wie zu erwarten, nicht nur reichlich Erythrozyten und Leukozyten in den großen Gefäßen und im sinusoidalen Netzwerk, sondern auch Thromben in den großen Gefäßen.

Im letzen Schritt **(Manuskript III in Vorbereitung)** konnten wir in einem präliminären Experiment zeigen, daß durch eine lokale Heparinisierung die Thrombenbildung effizient verhindert wurde. Die Tiere verstarben jedoch an lethalen Sickerblutungen aus der Basis des dezellularisierten Leberlappens, dort wo dieser zuvor abgeklemmt worden war. Vor Versuchen zur Repopulierung ist somit der nächste Schritt das beste Verfahren zur Verhinderung der Blutgerinnung im Lebergerüst zu finden, was das Blutungsrisiko nicht erhöht.

Schlussfolgerungen:

Der linkslateralen Leberlappens ist für die selektive in vivo Leberperfusion geeignet ist. In diesem Modell erwies sich 1%SDS als bestes Detergenz für die in-vivo Dezellularisierung.. Wir konnten zeigen, daß die Bauchorgane erfolgreich durch die gezielte Abdeckung mit einem PVDC-Film und trockenen Kompressen sowie der Platzierung eines Absaugkatheters von SDS abgeschirmt und damit von einer korrosiven detergenzbedingten Schädigung bewahrt werden können. Somit haben wir erfolgreich ein Überlebensmodell zur selektiven in-vivo Dezellularisation entwickelt.

Vor Versuchen zur Repopulierung ist der nächste Schritt das beste Verfahren zur Verhinderung der Blutgerinnung im Lebergerüst zu finden, was das Blutungsrisiko nicht erhöht.

Summary

Background:

Recently biological liver engineering was proposed as a novel strategy to generate transplantable organs and is actively pursued worldwide. Liver engineering basically consists of generation of an acellular scaffold followed by repopulation of the scaffold. Most researchers focus on ex-vivo liver engineering. However, despite the development of numerous protocols for decellularization, much less is known about successfully repopulating a scaffold. First, but rather preliminary reports were published describing selected in-vivo functions within a maximal observation time of 72h after transplanting the repopulated liver lobes. Long term function of a bioengineered full-size liver graft is still a vision of future. An alternative to ex-vivo liver engineering is needed to better understand functional repopulation. Recently, the research group of Pan (2016) reported in-vivo decellularization and recellularization on the right inferior lobe in rats. However, they sacrificed all experimental animals intraoperatively after an observation time of only 6 hours due to the suspected tissue injury caused by the detergent.

Aim:

The aim of this study is to generate a survival model of in-vivo selective liver lobe decellularization in rats.

Methods and Results:

As described in **manuscript I (JOVE 2018, IF 1.3)**, prior to perform in-vivo decellularization, we generated an in-vivo selective liver lobe perfusion model using the left lateral lobe. The selected liver lobe was perfused with heparin saline for either 20 min, 1 h, 2 h or 4 h respectively (n=3/group). Irrespectively of the perfusion time, the procedure was well tolerated by all animals (1w survival rate 100%, 12/12 animals). Histological assessment of the perfused lobe demonstrated the absence of blood cells in the portal vein branches, sinusoids and central vein branches already after 20min perfusion time, indicating successful generation of a circuit bypass through left lateral lobe in-vivo .

As described in **manuscript II (submitted to Acta Biomaterialia, IF 6.3)**, we compared three different protocols to identify the optimal protocol for in-vivo liver lobe decellularization. We observed that only using 2 hours of 1% SDS rather than 1% Triton X100 or 1% Triton X100 followed by 1% SDS resulted in the complete removal of cellular components as confirmed by histological assessment. We further characterized the scaffold

generated by the optimal protocol using 1% SDS. The integrity of the vascular structure including portal vein, hepatic artery, bile duct and central vein, as well as the micro- and ultrastructure of the matrix was confirmed by CT, histology and SEM, respectively. The main matrix proteins including collagen I and IV, elastin, fibronectin, and laminin were preserved as detected with strong signals in immunohistochemistry, altogether confirming the generation of a well-preserved high quality scaffold.

Additionally, we compared two methods to drain the waste fluid. Covering the abdominal organs with polyvinylidene chloride (PVDC) film and dry gauze together with placing an aspiration tube resulted in complete protection from the corrosive detergent. All animals reached the designed observation time of one week (n=6/6), in contrast to only 16.7% (n=1/6) using the other drainage method with only PVDC film + dry gauze.

Lastly, we further assessed the physiologically blood reperfusion of the scaffold. We found that blood cells but also some clots were visible in the portal vein, hepatic artery, sinusoids and central vein of the acellular scaffold confirmed by histological assessment 12 hours postoperatively.

We achieved first preliminary results (**manuscript III in preparation**) regarding the next step towards in-vivo liver engineering, the prevention of coagulation within the scaffold upon blood reperfusion. Testing layer-by-layer heparinization confirmed the effectiveness, but revealed that lethal bleeding occurred unavoidably (n=6/6) at the base of the decellularized liver lobe where the clamp was placed. Our next step prior to repopulating the scaffold will be directed to identify the optimal coating preventing coagulation without increasing the risk of bleeding.

Conclusions:

We concluded that using the left lateral lobe as the targeted liver lobe for in-vivo selected liver perfusion is technically feasible. We also concluded that using 1% SDS as detergent was optimal for in-vivo perfusion decellularization of targeted liver lobe. We further identified that covering the abdominal organs with PVDC, gauze and placing a suction tube is the most efficient way to prevent corrosive injury of the abdominal organs. Finally, we concluded that the physiological reperfusion of the in-vivo scaffold is feasible. Altogether it lays a solid foundation for further studying in-vivo liver engineering. Here the next challenge prior to repopulation is to achieve the balance between prevention of coagulation without provoking bleeding.

Introduction

Biological liver engineering is a new strategy to generate potentially transplantable liver grafts. Liver engineering consists of two steps: Generation of an acellular scaffold followed by repopulation. Liver scaffolds are usually generated by ex-vivo perfusion of the organ with biochemical detergents. The scaffolds are reseeded with either mature cells, hepatocellular as well as endothelial cell lines or mesenchymal stem cells. The three dimensional structure of the scaffold is available for cell adhesion, growth, differentiation, proliferation and migration, molecules signaling and promoting the expression of liver-specific functions.

Most of researchers focus on ex-vivo liver engineering. However, in previous studies, partially repopulated scaffolds [Bao 2011 and Jiang 2014] or engineered full liver grafts [Uygun 2010, Kadota et al 2014, Ko et al 2015, Bruinsma 2015, Bao 2015 and Hussein 2016] were transplanted as an auxiliary heterotopic graft. The maximal reported survival time was limited to 72 hours [Bao 2011]. To our knowledge, orthotopic transplantation of a repopulated full liver graft has not yet been performed or published. Long term function and transplantation of engineered organs is still in its infancy. Therefore, an alternative approach to ex-vivo liver engineering is needed.

The new concept of in-vivo organ-engineering emerged recently. This technique allows in-vivo repopulated partial liver scaffold to be subjected to in-vivo physiological blood perfusion with the unique advantage of physiological “culture” conditions including the maintenance of proper temperature, sufficient supply of oxygen and nutrients and growth factors. Furthermore, hepatic function of the remaining normal liver principally allows long term survival of the animal. Therefore, in-vivo liver engineered tissue can potentially serve as an in-vivo three dimension “cell culture” model for hepatocyte proliferation and stem cell differentiation in comparison with ex-vivo.

The group of Pan and colleagues were the first group to attempt in-vivo decellularization and repopulation using a rat model [Pan 2016]. They reported their novel technique of in-vivo decellularization of a single liver lobe followed by in-vivo repopulation using rat hepatocytes. However, the in-vivo surgical perfusion model of Pan has disadvantages. They achieved single liver lobe perfusion in rats at the expense of completely blocking the portal vein and inferior vena cava, which may cause severe harm to the animal. The experimental rats were sacrificed after only 6 hours of intraoperative observation time. They also claimed that the

short lifespan of the animals may be due to the injury caused by the detergent used. Postoperative survival has not yet been reported by now. Therefore, the in-vivo liver lobe perfusion technique needs further improvement to achieve postoperative survival. No study was identified up to now which successfully circumvented this problem. Maintenance of hepatic blood flow requires preservation of blood flow through the vena cava and through branches of the portal vein during the procedure of selective in-vivo decellularization and recellularization. This is needed to maintain systemic blood circulation and the perfusion of the undecellularized liver lobe. Measures to prevent corrosive injury by the detergent are also needed.

Therefore, despite substantially anatomic and technical challenges, we generated a survival model of in-vivo selective liver lobe decellularization based on our previous studies regarding hepatic anatomy of rat [Madrahimov 2006], portal vein cannulation technique for haemodynamic monitoring in mice [Xie 2014], and ex-vivo liver decellularization [Mussbach 2016, Mussbach et al 2016].

Hypothesis

Based on the described considerations we raise the following hypothesis:

- The selective left lateral lobe is a suitable lobe for in-vivo liver lobe perfusion in rats due to its vascular anatomy.
- Liver lobe decellularization in-vivo results in the complete removal of all cellular components within 2h.
- Perfusion decellularization with 1% SDS results in the multiscale preservation of the hepatic architecture and in the preservation of the protein composition of the scaffold.
- Complete protection of the abdominal organs from the corrosive detergent enables long term survival of the animals.
- Physiologically reperfusion of an in-vivo intact decellularized liver lobe is feasible.

Aims

We set five aims for this study:

- To establish a novel surgical technique for in-vivo selective left lateral liver lobe perfusion in rat.
- To identify the optimal protocol for in-vivo liver lobe perfusion decellularization.
- To confirm the integrity of structural architecture of the scaffold generated with the optimal protocol.
- To identify the optimal drainage method for in-vivo liver lobe perfusion decellularization.
- To confirm the physiological reperfusion of the in-vivo biological scaffold.

Study Design

In order to reach the aims we designed a study composed of two parts including five corresponding steps:

Part I → Manuscript I

- Establishment of a surgical technique for in-vivo perfusion only through the selective left lateral liver lobe in rat.

Part II → Manuscript II

- Comparison of three different detergents to identify the optimal protocol for in-vivo liver lobe decellularization in rat.
- Characterization of the scaffold generated with the optimal detergent.
- Comparison of two different drainage methods to identify the optimal drainage method for in-vivo liver lobe decellularization in rat.
- Physiological reperfusion of the intact decellularized liver lobe.

Manuscripts

Manuscript I

A novel surgical technique as a foundation for in-vivo partial liver engineering in rat

---

An Wang, Isabel Jank, Weiwei Wei, Claudia Schindler, and Uta Dahmen1

Journal of Visualized experiments; 6, October 2018.

doi:10.3791/57991 (2018).

https://www.jove.com/video/57991/a-novel-surgical-technique-as-foundation-for-vivo-partial-liver

Authorship

First author

Authors' Contribution

An Wang and U. Dahmen contributed to conception and design, as well as for critical revision of the article;

Isabel Jank: Assistance in editing the film and analyzing the results;

Weiwei Wei: Instruction regarding micro-surgical skills;

Claudia Schindler: Instruction regarding the hemodynamics of liver in rat.

Uta Dahmen: Supervision of the project.

jove Journal of Visualized Experiments www.jove.com

Video Article

A Novel Surgical Technique As a Foundation for *In Vivo* Partial Liver Engineering in Rat

An Wang[1], Isabel Jank[1], Weiwei Wei[1], Claudia Schindler[1], Uta Dahmen[1]

[1]Experimental Transplantation Surgery, Department of General, Visceral and Vascular Surgery, University Hospital Jena

Correspondence to: Uta Dahmen at Uta.Dahmen@outlook.com

URL: https://www.jove.com/video/57991
DOI: doi:10.3791/57991

Keywords: Bioengineering, Issue 140, *in vivo*, liver perfusion, left lateral lobe, cell culture system, decellularization, recellularization, liver engineering

Date Published: 10/6/2018

Citation: Wang, A., Jank, I., Wei, W., Schindler, C., Dahmen, U. A Novel Surgical Technique As a Foundation for *In Vivo* Partial Liver Engineering in Rat. *J. Vis. Exp.* (140), e57991, doi:10.3791/57991 (2018).

Abstract

Organ engineering is a novel strategy to generate liver organ substitutes that can potentially be used in transplantation. Recently, *in vivo* liver engineering, including *in vivo* organ decellularization followed by repopulation, has emerged as a promising approach over *ex vivo* liver engineering. However, postoperative survival was not achieved. The aim of this study is to develop a novel surgical technique of *in vivo* selective liver lobe perfusion in rats as a prerequisite for *in vivo* liver engineering. We generate a circuit bypass only through the left lateral lobe. Then, the left lateral lobe is perfused with heparinized saline. The experiment is performed with 4 groups (n = 3 rats per group) based on different perfusion times of 20 min, 2 h, 3 h, and 4 h. Survival, as well as the macroscopically visible change of color and the histologically determined absence of blood cells in the portal triad and the sinusoids, is taken as an indicator for a successful model establishment. After selective perfusion of the left lateral lobe, we observe that the left lateral lobe, indeed, turned from red to faint yellow. In a histological assessment, no blood cells are visible in the branch of the portal vein, the central vein, and the sinusoids. The left lateral lobe turns red after reopening the blocked vessels. 12/12 rats survived the procedure for more than one week. We are the first to report a surgical model for *in vivo* single liver lobe perfusion with a long survival period of more than one week. In contrast to the previously published report, the most important advantage of the technique presented here is that perfusion of 70% of the liver is maintained throughout the whole procedure. The establishment of this technique provides a foundation for *in vivo* partial liver engineering in rats, including decellularization and recellularization.

Video Link

The video component of this article can be found at https://www.jove.com/video/57991/

Introduction

The indications for organ transplantation are constantly expanding. In contrast, organ donation rates and overall quality of organs are declining, leading to an increasing demand for grafts. The number of candidates added to the liver transplant waiting list continued to increase (*e.g.*, in the United States, 11,340 patients were added in 2016, compared with 10,636 in 2015)[1]. Despite substantial efforts, the number of available organs does not meet clinical needs. Due to the increased incidence of liver disease, many patients with end-stage liver diseases die on the transplant waiting list before a donor organ becomes available. To meet the huge demand for donor liver grafts, alternative approaches using liver tissue engineering principles are being actively pursued[2]. Nowadays, a newly developed biological technique of liver engineering could potentially overcome this shortage.

Liver engineering consists of two steps: the generation of an acellular scaffold, followed by a repopulation of the scaffold. To obtain a biological acellular liver scaffold, the explanted liver is perfused *via* the vascular system with ionic or nonionic detergents, which can remove the cellular material from the liver. In most previous studies, a biological acellular liver scaffold was achieved by perfusion of the liver with a combination of sodium dodecyl sulfate and TritonX100. As a result, all cells were removed, whereas the structure of the extracellular matrix was maintained. The organ scaffolds were reseeded with mature cells, hepatocellular, as well as endothelial cell lines, and primary hepatocytes with or without the simultaneous application of endothelial cells or mesenchymal stem cells (MSC). Most researchers focus on *ex vivo* liver engineering[3,4,5,6,7,8,9,10,11,12,13,14]. However, in most previous studies, only small pieces of repopulated scaffold cubes were transplanted into different heterotopic implantation sites. In a few studies, partial repopulated scaffolds were transplanted as an auxiliary graft. However, the maximal reported survival time was only 72 h[8,14]. As far as we know, orthotopic transplantation of a repopulated full liver graft has not yet been performed or published about. The long-term function and transplantation of engineered organs are still in their infancy. Therefore, an alternative approach to *ex vivo* liver engineering is needed.

In vivo liver engineering may represent an alternative to study hepatic repopulation under physiological conditions. The advantages of *in vivo* liver engineering compared to *ex vivo* liver engineering are manifold. The *in vivo* repopulated partial liver scaffold is subjected to physiological blood perfusion with proper temperature, sufficient oxygen, nutrients, and growth factors in contrast to *ex vivo* perfusion with artificial culture medium. Furthermore, the remaining partial normal liver maintains the hepatic function, principally allowing long-term survival. Since an implanted *ex vivo* engineered liver graft is still incapable of sustaining the long-term survival of experimental animals by its liver function[8], we

envision that *in vivo* partial liver engineeringwould ultimately become a promising model to further study the evolution of engineered livers with longer survival observations than *ex vivo*.

Recently, one research group (Pan and colleagues) presented, for the first time, a technique of *in vivo* liver engineering[15]. They achieved the isolated perfusion of the right inferior liver lobe in living rats despite anatomic and technical challenges. They reported the first intraoperative results of *in vivo* repopulation using a rat primary hepatocyte cell line. However, the *in vivo* surgical perfusion model of Pan *et al.* has disadvantages. They achieved single liver lobe perfusion in rats at the expense of completely blocking the portal vein and inferior vena cava, which may cause severe harm to the animal. The experimental rats were sacrificed after only 6 hours of intraoperative observation time. Therefore, the *in vivo* liver lobe perfusion technique needs further improvement to achieve postoperative survival.

We developed a novel survival model for *in vivo* liver lobe perfusion, based on previous studies of the hepatic anatomy of rat[16], the portal vein cannulation technique for hemodynamic monitoring in mice[17], and liver bioengineering[18,19]. The key steps for the procedure are illustrated in **Figure 1A** - **1E**.

This technique is suitable for those who want to use this experimental *in vivo* perfusion model for basic research on partial organ treatment by infusion with drugs, *in vivo* decellularization as a chemical resection for organ diseases (*e.g.*, liver cancer), *in vivo* cell culture in a decellularized matrix comparing *ex vivo* two-dimensional and three-dimensional cell culture systems[20,21,22,23,24,25,26], and *in vivo* liver engineering by decellularization and repopulation.

Protocol

The housing and all procedures carried out were in accordance with German animal welfare legislation. All gauze, covering clothes, and surgical instruments are autoclaved and prepared before the operation. All procedures are carried out under sterile conditions.

1. Preparation of the Rat for the Surgical Procedure

1. Place the rat in an induction chamber and anesthetize the rat with 4% vaporized isoflurane and 100% oxygen at 0.5 L/min for about 3 min, until the rat is completely anesthetized.
2. Take the rat out of the induction chamber and measure its body weight.
3. Shave the fur of the surgical region on the abdomen.
4. Place the animal back into the isoflurane chamber for an additional 2 min to deepen anesthesia.
5. Place the rat on the operation table in supine position.
6. Fix the anesthesia mask to the mouth region of the rat and keep the animal anesthetized with a continuous gas flow of 2% vaporized isoflurane and 100% oxygen at a flow rate of 0.5 L/min.
7. Fix the limbs with pieces of tape.
8. Apply vet ointment on both eyes to prevent dryness.
9. Administer buprenorphine 0.05 mg/kg subcutaneously, to relieve pain during the operation period.
10. Disinfect the surgical field of the abdomen with 3 rounds of iodine tincture followed by 2 rounds of 70% alcohol.
11. Place sterilized gauze around the area where the incision will be made to only leave the operation field of the abdomen exposed.
12. Proceed to perform the operation when the toe-pinch withdrawal reflex of the rat is absent.

2. Laparotomy of the Rat

1. Make a transverse abdominal skin and muscle incision using scissors and an electrical coagulator.
2. Fix and pull the xiphoid process toward the head using a 4-0 polypropylene suture.
   NOTE: Pay attention to lift up the xiphoid process vertically to better expose the liver, but proceed with caution to avoid severe respiratory restriction and suffocation.
3. Open the peritoneal cavity by pulling both sides of the abdominal walls towards the head with two subcostal hooks to expose the liver.
4. Cover the duodenum and small intestine in the abdominal cavity with a moistened gauze to avoid drying.
5. Lift left and right median lobes up by using a moistened gauze and hold them against the thorax to better expose the hilum of the liver.
6. Place the rat under a stereomicroscope (8X magnification).
7. Drop some warm saline into the abdomen and onto the surface of the liver and intestines every several minutes, to prevent drying during the whole procedure.

3. Establishment of a Bypass Passage Within the Left Lateral Lobe

1. Dissect the left portal vein and ligate it with a 6-0 silk suture at the base (**Figure 2A**).
2. Block the left hepatic artery, the left bile duct along with the left median portal vein, the left median hepatic artery, and the left median bile duct with micro clamps to prevent a flow of the perfusate to the left median lobe (**Figure 2B**).
3. Separate the left lateral lobe by cutting off the surrounding ligaments of the lobe with micro scissors.
4. Block the left lateral hepatic vein by clamping at the base of the left lateral lobe with micro clamps (**Figure 2C**).
   NOTE: Make sure not to clamp the left portal vein as well by mistake.
5. Use mosquito clamps to hold the ligature of the left portal vein and keep the vein with proper tension for later cannulation.
6. Carefully make an incision in the front wall of the left portal vein by puncturing it with a 24-G needle-dwelling catheter (**Figure 3A**).
   NOTE: To create a bypass, vascular access points on the left portal vein and the left hepatic vein are needed. For this step, it is preferred to create the vascular access by puncturing the vessels with a needle rather than making a larger incision using scissors. This reduces the risk of bleeding and later stenosis.
7. Withdraw the catheter and take the needle out of the catheter to obtain a needle-free 24-G catheter.

8. Connect the catheter to a perfusion tube, of which the other endpoint connects to a 20-mL syringe with 15 mL of 40 U/mL heparinized saline on a perfusion pump.
9. Turn on the pump for perfusing the tube to expel air out from the tube and the needle-free catheter.
10. Turn off the perfusion pump.
11. Again, insert the needle-free catheter into the left portal vein *via* the punctured incision on the vein (**Figure 3B**).
    NOTE: Owing to the fact there is very limited space for fixing the catheter, it is not fixed at this point. Therefore, the surgeon should use care to avoid the displacement of the cannulated catheter.
12. Carefully make another incision at the margin of the exposed region of the left lateral hepatic vein by puncturing it with a 22- or 24-G needle-dwelling catheter (**Figure 3C**).
    NOTE: It is recommended that the catheter be slightly smaller than the vessel.
13. Withdraw the catheter and take the needle out of the catheter to obtain a needle-free 22-G catheter.
14. Turn on the perfusion pump to perfuse heparinized saline into the left lateral lobe *via* the 24-G cannulated needle-free catheter of the left portal vein at a flow rate of 0.5 mL/min.
15. Use dry gauze to absorb out-flowing waste fluid around the incision area of the left lateral hepatic vein.
16. Cannulate the left lateral hepatic vein *via* the punctured incision of the vein with the 22-G needle-free catheter, to generate a fluid outlet to minimize intra-abdominal contamination (**Figure 3D**).
    NOTE: It is technically difficult to fix the cannulated catheter to the liver lobe. Therefore, the surgeon should pay attention to avoid displacement of the catheter. Alternatively, without cannulation of the left lateral hepatic vein with a catheter, waste fluid can also be absorbed at the incision region of the vein only with a dry gauze.
17. Keep perfusing the left lateral lobe with heparinized saline for around 20 min (group 1) and then only with saline for 2 h, 3 h, or 4 h (group 2, group 3, and group 4, respectively).
18. Turn off the pump to stop the perfusion.

4. Physiological Reperfusion of the Left Lateral Lobe

1. Take off both catheters from the left portal vein and the left lateral hepatic vein.
2. Close the incision of the left portal vein with an 11-0 polyamide suture.
3. Close the incision of the left lateral hepatic vein with an 11-0 polyamide suture as well.
4. Unclamp the left lateral hepatic vein.
5. Unclamp the left median portal vein, left bile duct, and left hepatic artery.
6. Cut off the ligature on the left portal vein to reopen the vein.

5. Closure of the Abdominal Wall

1. Close the muscle layer of the abdominal wall by interrupted suturing with a 4-0 absorbable polyglactin 910 suture.
2. Close the skin layer of the abdominal wall by interrupted suturing with a 4-0 absorbable polydioxanone suture.
3. After closing the abdomen, disinfect the skin incision with 70% alcohol.

6. Postoperative Treatment of the Rat

1. Place the animal on a warming pad for resuscitation for about 10 min and then put it into a new cage.
2. Administer buprenorphine 0.05 mg/kg subcutaneously 2x a day for a consecutive 3 d postoperatively to release pain.

Representative Results

Twelve male (aged 12 - 13 weeks) Lewis rats were used to assess the effect of selective liver lobe perfusion. The experiment was performed in four groups (n = 3 rats per group). Using different perfusion periods of 20 minutes, 2 hours, 3 hours, and 4 hours, following the steps described above, we successfully achieved *in vivo* single lobe perfusion.

***In Vivo* Perfusion of the Left Lateral Lobe:**

The accurate anatomical identification of the left portal vein and the left lateral hepatic vein and the successful left portal vein and left lateral hepatic vein cannulation can be confirmed after perfusion with heparinized saline. The first indicator of a successful identification and cannulation was the observation that blood mixed with perfusate was flowing out of the left lateral lobe *via* the fluid outlet (**Figure 4A**). The successful surgical perfusion model was further confirmed by observing the change of the left lateral lobe's color after the perfusion with heparinized saline. The color of the left lateral lobe changed from bright red to faint yellow, indicating the removal of blood from the left lateral lobe. To confirm the maintenance of the physiological perfusion of the remaining lobes, the color of the remaining liver lobes was constantly observed during the perfusion of the left lateral lobe. The correct perfusion of the left lateral lobe resulted in the lobe turning faint yellow while the remaining liver lobes maintained their bright red color throughout the whole process (**Figure 4B**).

Physiological Reperfusion of the Left Lateral Lobe:

To assess the patency of the cannulated vessels after closing the incisions of the vessels and reopening the vessels, the color change of the left lateral lobe was observed. A few red spots appeared on the surface of the perfused faint yellow left lateral lobe after reopening the left lateral hepatic vein, indicating initial retrograde perfusion in the left lateral lobe (**Figure 5A**). The surface of the targeted lobe later showed even more red spots after releasing the micro clamps of the left hepatic artery, left bile duct, and left median portal vein, implying further physiological perfusion of the left lateral lobe *via* the reopened vessels (**Figure 5B**). The surface of the targeted liver lobe turned dark red after reopening the left portal vein, confirming that the targeted liver lobe regained its full physiological perfusion *via* the left portal vein (**Figure 5C**).

Histology of the Perfused Left Lateral Lobe:

After finishing heparinized saline or saline perfusion, the selectively perfused left lateral lobe (as experimental) and the normal inferior caudate lobe (as control) were resected and fixed with formaldehyde and then subjected to a histological examination (H&Estaining). In the left lateral lobe, there are no obvious blood cells visible in the branch of the portal vein, sinusoids, and central vein. As expected, red cells were visible in the branch of the hepatic artery (**Figure 6A** and **6C**). In the normal inferior caudate lobe (as control), blood cells were significantly observed in the branch of the portal vein, the sinusoids, and the central vein (**Figure 6B** and **6D**).

Survival Rate:

Twelve out of twelve experimental rats resulted in a 1-week survival rate of 100%. However, 3 experimental rats which underwent 4 hours of perfusion suffered temporarily from diarrhea and bloody discharge from the eyes on the second or third day postoperatively.

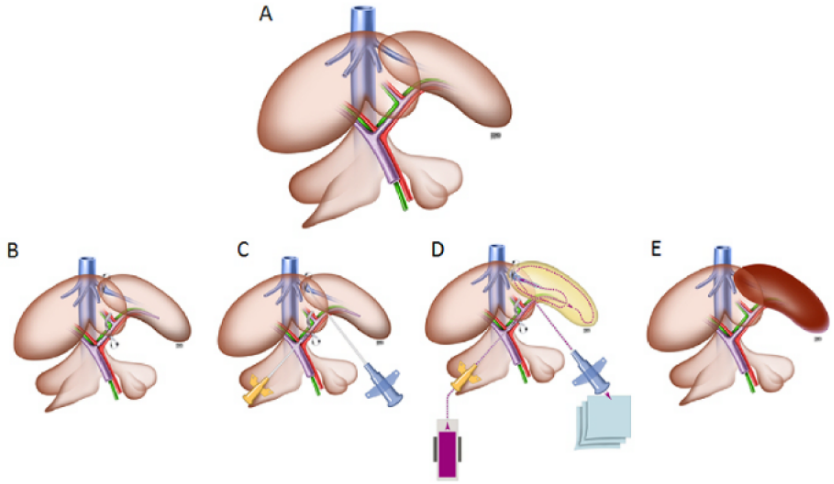

Figure 1: Scheme of the surgical *in vivo* single liver lobe perfusion model. (**A**) This is a schematic drawing of the rat liver anatomy.(**B**) This panel shows the blockage of the left portal vein, the left hepatic artery, the left bile duct, the left median portal vein, and the left lateral hepatic vein. (**C**) This panel shows the cannulation of the left portal vein and the left lateral hepatic vein with catheters for fluid inlet and outlet. (**D**) This panel shows the perfusion of the left lateral lobe with heparinized saline by a perfusion pump. (**E**) This panel shows the physiological reperfusion of the left lateral lobe after reopening the blocked vessels to the lobe. Please click here to view a larger version of this figure.

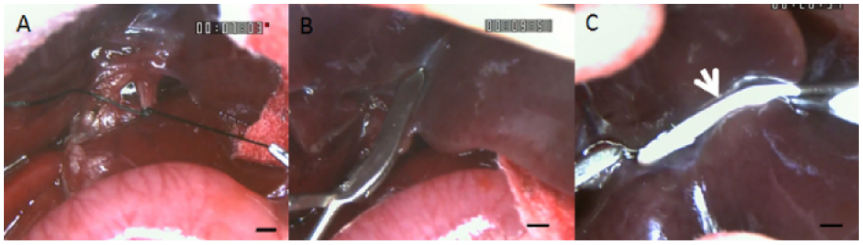

Figure 2: Intraoperative images showing the blockage of the vessels supplying and draining the left lateral lobe. (**A**) This panel shows the ligation of the left portal vein. (**B**) This panel shows the blockage of the left hepatic artery, the left bile duct, and the left median portal vein/ hepatic artery/bile duct with micro clamps. (**C**) This panel shows the blockage of the left lateral hepatic vein with micro clamps (white arrow). The scale bars are 1 mm. Please click here to view a larger version of this figure.

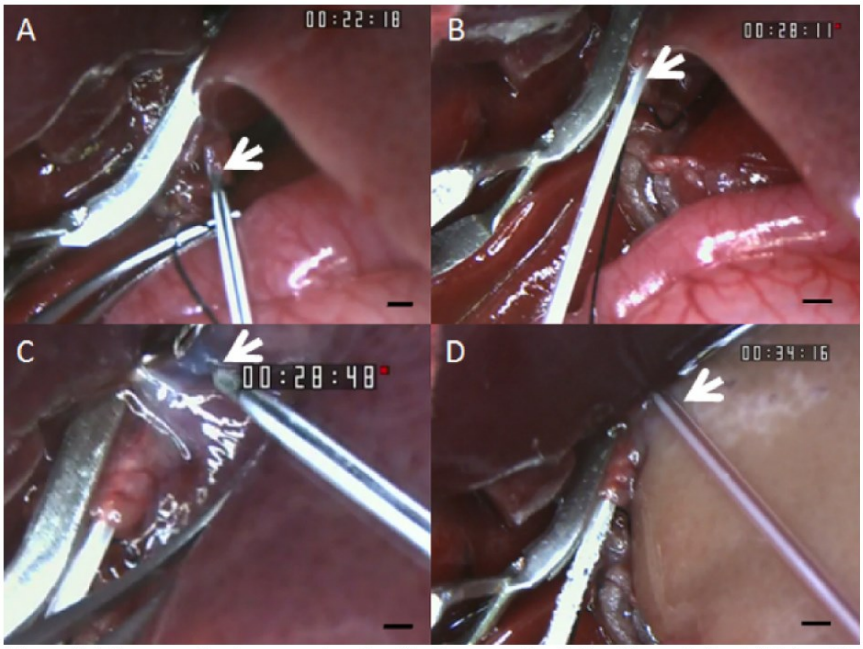

Figure 3: Intraoperative images showing the bypass circulation through the left lateral lobe. (**A**) This panel shows the incision in the left portal vein (white arrow) by puncturing it with a 24-G needle-dwelling catheter. (**B**) This panel shows the cannulation of the left portal vein for a fluid inlet with a 24-G needle-free catheter (white arrow). (**C**) This panel shows the incision in the left lateral hepatic vein (white arrow) by puncturing it with a 22-G needle-dwelling catheter. (**D**) This panel shows the cannulation of the left lateral hepatic vein for a fluid outlet with a 22-G needle-free catheter (white arrow). The scale bars are 1 mm. Please click here to view a larger version of this figure.

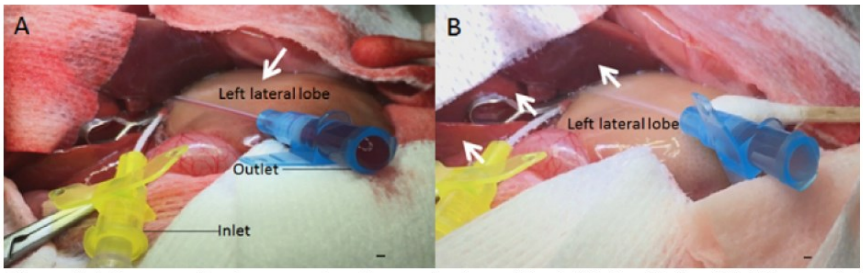

Figure 4: Intraoperative images showing perfusion of the left lateral lobe. (**A**) This panel shows perfusate flowing into the left lateral lobe *via* the inlet (yellow catheter) and flowing out of the left lateral lobe *via* the outlet (blue catheter). The left lateral lobe was, indeed, selectively perfused, as shown by the color changing of the lobe (white arrow). (**B**) Note the color change of the left lateral lobe to faint yellow after the perfusion with heparinized saline, while the remaining liver lobes remain bright red (white arrows). The scale bars are 1 mm. Please click here to view a larger version of this figure.

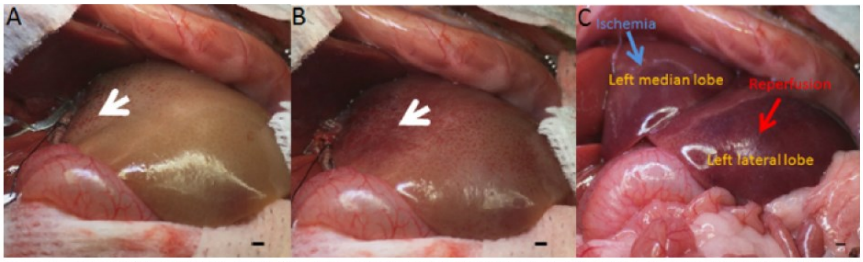

Figure 5: Physiological reperfusion of the left lateral lobe. (**A**) This panel shows the retrograde perfusion of the left lateral lobe after reopening the left lateral hepatic vein (white arrow). (**B**) This panel shows the physiological reperfusion of the left lateral lobe (white arrow) after releasing the micro clamps on the left median portal vein and the left hepatic artery. (**C**) This panel shows the complete reperfusion of the left lateral lobe (red arrow) after reopening the left portal vein and the ischemia of the left median lobe (blue arrow). The scale bars are 1 mm. Please click here to view a larger version of this figure.

jove Journal of Visualized Experiments www.jove.com

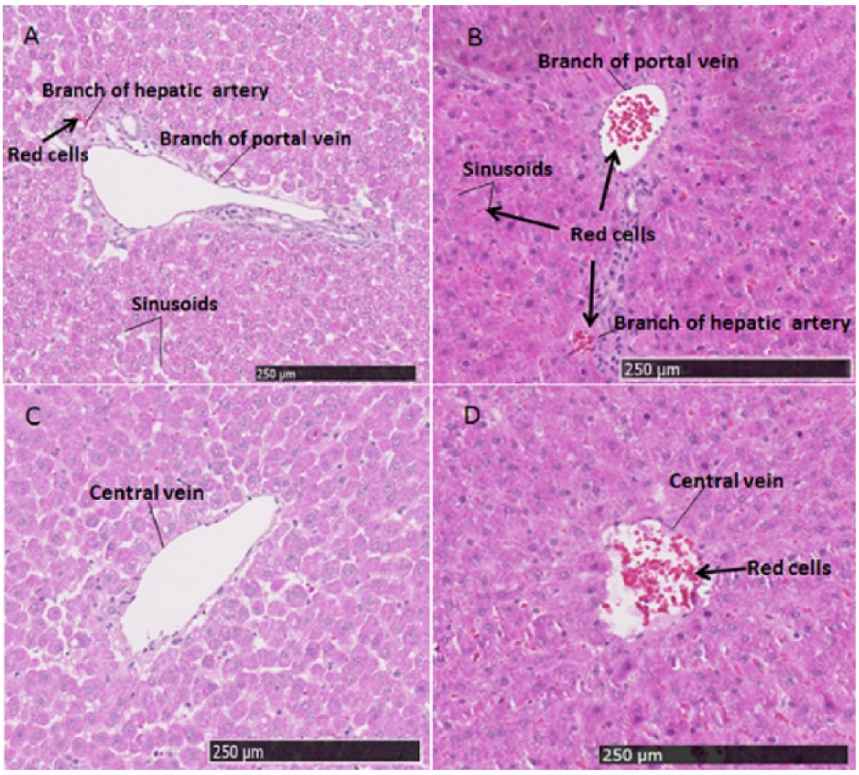

Figure 6: Histological assessments (H&E staining). (**A** and **C**) These panels show a histological assessment of the heparin-saline-perfused left lateral lobe (experimental lobe) demonstrating the absence of blood cells in **(A)** the portal vein and sinusoids, and (**C**) the central vein. (**A**) However, red cells are visible in the hepatic artery (black arrow) as expected. (**B** and **D**) These panels show a histological assessment of the normal inferior caudate lobe (control) revealing the presence of blood cells in all vascular structures: (**B**) portal vein, hepatic artery, and sinusoids (black arrows), and (**D**) central vein (black arrow). The scale bars are 250 µm.

Parameters	Results	
Research group	Pan et al 2016 [15]	Own group
In-vivo	Yes	Yes
Target liver lobe	Right inferior lobe 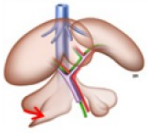	Left lateral lobe 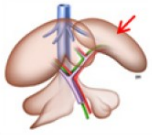
Blockage of vena cava and main portal vein	Yes 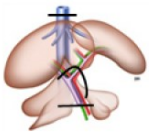	No 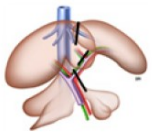
Ischemia of the remaining lobes	Yes	Only left median lobe
Cannulation of vena cava	Yes	No
Cannulation of main portal vein	Yes	No
Portal hypertension	Yes	No
1 week survival rate	Sacrificed intraoperatively	100%

Table 1. Comparison between different models of *in vivo* liver engineering. This table demonstrates critical differences in the two model establishments between Pan *et al.*[15] and our research group.

Discussion

By blocking and cannulating the left portal vein with a catheter as a fluid inlet and the left lateral hepatic vein with another catheter as a fluid outlet, we successfully generated an *in vivo* fluid bypass within the left lateral lobe, indicating that although the technique is highly challenging due to the small size of the vessels for cannulation and a high risk of causing bleeding, it is feasible. Even the rats undergoing a long perfusion period of 4 hours survived at least 1 week, showing that the rats could tolerate this surgical procedure.

In the following section, we describe the three technically most difficult and critical steps and how to successfully master them. Firstly, in the process of separation and ligation of the left portal vein, due to the close spatial relationship of the targeted portal vein with the surrounding liver parenchyma, isolation of the vessel has a high risk of causing bleeding. We recommend using micro forceps rather than scissors to separate the left portal vein, by carefully tearing apart the connected avascular tissue surrounding the left portal vein. Secondly, in terms of the incision on the front wall of the left portal vein, an oversize incision on the front wall of the left portal vein may increase the difficulty of incision repair and the chance of causing stenosis after vascular anastomosis. We recommend using a needle-dwelling catheter instead of scissors for making a properly sized incision. Thirdly, regarding the blockage of the left lateral hepatic vein, if the exposed region of the left lateral hepatic vein is blocked improperly, there will not be sufficiently exposed space on the left lateral hepatic vein for later cannulation. We suggest the clamping should be performed close to the left median lobe rather than in the middle of the exposed region of the left lateral hepatic vein.

We compare the two models of selective *in vivo* liver perfusion between Pan *et al.*[15] and ours (**Table 1**). Firstly, the selection of the targeted liver lobe is considered a most critical step for the model establishment. We selected a rather isolated lobe, the left lateral lobe, as the targeted lobe for *in vivo* surgical perfusion model establishment. In contrast, the research group of Pan selected the right inferior lobe for the model[14]. Shortcomings of selecting the right inferior lobe are as followings: firstly, they had to compromise by completely blocking and cannulating the vena cava for a fluid outlet, which may negatively impact the blood circulation of the animal. Secondly, they had to block and cannulate the main portal vein for an inlet, which caused ischemia of the remaining liver lobes, and portal hypertension. As compared to the lobe targeted here, the left lateral lobe, we blocked and cannulated left lateral hepatic vein instead of the vena cava for a fluid outlet. We generated a fluid inlet by selecting the left portal vein, which has a rather large diameter, facilitating dissection, blockage, and cannulation. Therefore, directly blocking the blood flow to the vena cava and the main portal vein is avoided in the model presented here, which is critical to the survival of the rat.

Despite the great potential for *in vivo* liver lobe perfusion, this technique has some limitations. Firstly, ischemia of the left medial lobe is inevitable, due to the blockage of the left median portal vein during the process. Secondly, based on the temporary blockage at the base of the left lateral lobe using micro clamps, this may lead to damage of the liver parenchyma surrounding the lobar base and inevitably cause a slight leakage during the perfusion with heparinized saline. Three experimental rats which were subjected to a perfusion period of 4 hours suffered temporarily from diarrhea and bloody ocular discharge, suggesting that 4 hours might be the maximum perfusion period for a rat without suffering more complications. To our knowledge, at least 3 hours is required for the decellularization of a whole rat liver *ex vivo*[18]. Therefore, the 4 hours of perfusion time we intended to achieve would be sufficient for further liver lobe decellularization, which is a prerequisite for liver engineering by cell repopulation of a liver scaffold.

In the future, this novel technique for an *in vivo* perfusion model may potentially be used in experimental research for partial organ treatment by infusion with drugs, in *in vivo* partial organ decellularization as chemical resection, as an "*in vivo* cell culture system", and, possibly most importantly, for *in vivo* partial organ engineering.

Disclosures

The authors have nothing to disclose.

Acknowledgements

The authors would like to thank Jens Geiling from the Institute of Anatomy I, Jena University Hospital, for producing the schematic drawings of rat liver anatomy.

References

1. Kim, W. R. *et al.* OPTN / SRTR 2016 Annula Data Report: Liver. *American Journal of Transplantation.* **Suppl 1**, 172-253 (2018).
2. Palakkan, A.A., Hay, D.C., Anil Kumar, P.R., Kumary, T.V., Ross, J.A. Liver tissue engineering and cell sources: issues and challenges. *Liver International.* **33**, 666-676 (2013).
3. Hynes, R.O. The extracellular matrix: not just pretty fibrils. *Science.* **326**, 1216-1219 (2009).
4. Flaim, C.J., Chien, S., Bhatia, S.N. An extracellular matrix microarray for probing cellular differentiation. *Nature Methods.* **2**, 119-125 (2005).
5. Wells, R.G. The role of matrix stiffness in regulating cell behavior. *Hepatology.* **47**, 1394-1400 (2008).
6. Ren, H. *et al.* Evaluation of two decellularization methods in the development of a whole-organ decellularized rat liver scaffold. *Liver International.* **33**, 448-458 (2013).
7. Yagi, H. *et al.* Human-scale whole-organ bioengineering for liver transplantation: a regenerative medicine approach. *Cell Transplantation.* **22**, 231-242 (2013).
8. Jiang, W.C. *et al.* Cryo-chemical decellularization of the whole liver for mesenchymal stem cells-based functional hepatic tissue engineering. *Biomaterials.* **35**, 3607-3617 (2014).
9. Uygun, B.E. *et al.* Organ reengineering through development of a transplantable recellularized liver graft using decellularized liver matrix. *Nature Medicine.* **16**, 814-820 (2010).

10. Baptista, P.M. *et al.* The use of whole organ decellularization for the generation of a vascularized liver organoid. *Hepatology.* **53**, 604-617 (2011).
11. Bruinsma, B.G., Kim, Y., Berendsen, T.A., Yarmush, M.L., Uygun, B.E. Layer-by-layer heparinization of decellularized liver matrices to reduce thrombogenicity of tissue engineered grafts. *Journal of Clinical and Translational Research.* **1** (1) (2015).
12. Park, K.M. *et al.* Decellularized Liver Extracellular Matrix as Promising Tools for Transplantable Bioengineered Liver Promotes Hepatic Lineage Commitments of Induced Pluripotent Stem Cells. *Tissue Engineering Part A.* **22**, 449-460 (2014).
13. Ko, I.K. *et al.* Bioengineered transplantable porcine livers with re-endothelialized vasculature. *Biomaterials.* **40**, 72-79 (2015).
14. Bao, J. *et al.* Construction of a portal implantable functional tissue-engineered liver using perfusion-decellularized matrix and hepatocytes in rats. *Cell Transplantation.* **20**, 753-766 (2011).
15. Pan, J. *et al.* In-vivo organ engineering: Perfusion of hepatocytes in a single liver lobe scaffold of living rats. *The International Journal of Biochemistry & Cell Biology.* **80**, 124-131 (2016).
16. Madrahimov, N. *et al.* Marginal hepatectomy in the rat: from anatomy to surgery. *Annals of Surgery.* **244**, 89-98 (2006).
17. Mussbach, F., Settmacher, U., Dirsch, O., Dahmen, U. Bioengineered Livers: A New Tool for Drug Testing and a Promising Solution to Meet the Growing Demand for Donor Organs. *European Surgical Research.* **57**, 224-239 (2016).
18. Mussbach, F., Settmacher, U., Dirsch, O., Dahmen, U. Liver engineering as a new source of donor organs: A systematic review. *Der Chirurg.* **87**, 504-513 (2016).
19. Xie, C. *et al.* Monitoring of systemic and hepatic hemodynamic parameters in mice. *Journal of Visualized Experiments.* (92), e51955 (2014).
20. Zhou, P. *et al.* Decellularization and Recellularization of Rat Livers With Hepatocytes and Endothelial Progenitor Cells. *Artificial Organs.* **40**, E25-E38 (2016).
21. Yagi, H. *et al.* Human-scale whole-organ bioengineering for liver transplantation: a regenerative medicine approach. *Cell Transplantation.* **22**, 231-242 (2013).
22. Otsuka, H., Sasaki, K., Okimura, S., Nagamura, M., Nakasone, Y. Micropatterned co-culture of hepatocyte spheroids layered on non-parenchymal cells to understand heterotypic cellular interactions. *Science and Technology of Advanced Materials.* **14**, 065003 (2013).
23. Bale, S.S. *et al.* Long-term coculture strategies for primary hepatocytes and liver sinusoidal endothelial cells. *Tissue Engineering Part C: Methods.* **21**, 413-422 (2015).
24. Wu, Q. *et al.* Optimizing perfusion-decellularization methods of porcine livers for clinical-scale whole-organ bioengineering. *BioMed Research International.* p. 785474 (2015).
25. Barakat, O. *et al.* Use of decellularized porcine liver for engineering humanized liver organ. *Journal of Surgical Research.* **173** (1), e11-25 (2012).
26. Navarro-Tableros, V. *et al.* Recellularization of rat liver scaffolds by human liver stem cells. *Tissue Engineering Part A.* **21** (11-12), 1929-1939 (2015).

Manuscripts

Manuscript II

A survival model of in-vivo partial liver lobe decellularization towards in-vivo liver engineering

---

Tissue Engineering Part C (accepted)

Accepted date: 27, Sept 2019.

Authorship

First author

Authors' Contribution

An Wang: Responsibility of designing and establishing the whole procedure, and analyzing the results and writing of the manuscript.

Olha Kuriata: Assistance in drainage for in-vivo perfusion decellularization and analyzing the results.

Fengming Xu: Assistance in DNA quantification for in-vivo perfusion decellularization and analyzing the results.

Isabel Jank: Assistance in the writing of the paper.

Sandor Nietzsche: Instruction regarding generation of the ultrastructural images of the scaffolds using Scanning electronic microscopy (SEM) technique and analysizing the results

Felix Gremse: Conduction and Instruction regarding the three-dimensional image construction of the scaffold using Micro-CT technique.

Olaf Dirsch: Assistance in interpernation of histological sections for in-vivo perfusion decellularization and analyzing the results.

Utz Settmacher: Instruction of liver anatomy of rat.

Uta Dahmen: Supervision of the project.

A survival model of in-vivo partial liver lobe decellularization towards in-vivo liver engineering

An Wang[1], *Olha Kuriata*[1], *Fengming Xu*[1], *Sandor Nietzsche*[2], Felix Gremse[3], Olaf Dirsch[4], Utz Settmacher[5], **Uta Dahmen**[1]

1. Experimental Transplantation Surgery, Department of General, Visceral and Vascular Surgery, Jena University Hospital, Germany

2. Center for Electron Microscopy, Jena University Hospital, Germany

3. Experimental Molecular Imaging, RWTH Aachen University, Germany

4. Institute of Pathology, Klinikum Chemnitz gGmbH, Germany

5. Department of General, Visceral and Vascular Surgery, Jena University Hospital, Germany

An Wang

Experimental Transplantation Surgery,

Department of General, Visceral and Vascular Surgery

Jena University Hospital

Jena, Germany

Wangan021@outlook.com

Olha Kuriata

Experimental Transplantation Surgery,

Department of General, Visceral and Vascular Surgery

Jena University Hospital

Jena, Germany

Olgakuryata@gmail.com

Fengming Xu

Experimental Transplantation Surgery,

Department of General, Visceral and Vascular Surgery

Jena University Hospital

Jena, Germany

Fengming.Xu@med.uni-jena.de

Sandor Nietzsche

Center for Electron Microscopy

Jena University Hospital

Jena, Germany

Sandor.Nietzsche@med.uni-jena.de

Felix Gremse

Experimental Molecular Imaging, RWTH Aachen University

Aachen, Germany

fgremse@ukaachen.de

Olaf Dirsch

Institute of Pathology

Klinikum Chemnitz gGmbH

Chemnitz, Germany

olaf.dirsch@gmail.com

Utz Settmacher

Department of General, Visceral and Vascular Surgery

Jena University Hospital

Jena, Germany

Utz.Settmacher@med.uni-jena.de

Corresponding author:

Prof. Dr. med. Uta Dahmen

1 Experimental Transplantation Surgery,

Department of General, Visceral and Vascular Surgery

Jena University Hospital

Jena, Germany

uta.dahmen@med.uni-jena.de

Abstract:

In-vivo liver decellularization has become a promising strategy to study in-vivo liver engineering. However, long term survival after in-vivo liver decellularization has not yet been achieved due to anatomical and technical challenges. This study aimed to establish a survival model of in-vivo partial liver lobe perfusion-decellularization in rat.

We compared three decellularization protocols (1%Triton X100 followed by 1%SDS, 1%SDS versus 1%Triton X100, n=6/group). Using the optimal one as judged by macroscopy,

histology and DNA-content, we characterized the structural integrity and matrix-proteins using histology, scanning electron microscopy (SEM), Computed Tomography (CT) scanning and immunohistochemistry. We prevented contamination of the abdominal cavity with the corrosive detergents by using polyvinylidene chloride (PVDC) film + dry gauze in comparison to PVDC-film + dry gauze + aspiration tube (n=6/group). Physiological reperfusion was assessed by histology. Survival rate was determined after a 7 d observation period.

Only perfusion with 1% SDS resulted in an acellular scaffold (fully translucent without histologically detectable tissue remnants, DNA concentration is less than 2% of that in native lobe) with remarkable structural and ultrastructural integrity as well as preservation of main matrix proteins (immunohistochemically positive for collagen IV, laminin, and elastin). Contamination of abdominal organs with the potentially toxic SDS-solution was achieved by placing a suction tube in addition to the PDVC-film + dry gauze and allowed 7d-survival of all animals without severe postoperative complications. Upon reperfusion, the liver turned red within sec without any leakage from the surface of the liver. About 12 h after reperfusion, blood cells but also some clots were visible in the portal vein (PV), sinusoidal matrix network and central vein (CV), suggesting physiological perfusion.

In conclusion, our results study shows the first available data on generation of a survival model of in-vivo parenchymal organ decellularization, creating a critical step towards in-vivo organ engineering.

Keywords

Perfusion decellularization in-vivo, Polyvinylidene chloride film, extracellular matrix, In-vivo liver engineering, In-vivo organ engineering

Abbreviations

BD: Biliary duct.

CV: Central vein

CT: Computed Tomography

HA: Hepatic artery,

HV: Hepatic vein

LLL: Left lateral lobe

RML: Right median lobe

IVC: Inferior vena cava,

PVDC: Polyvinylidene chloride

PV: Portal vein,

RML: Right median lobe

SDS: Sodium dodecyl sulfate

SEM: Scanning electron microscope

Impact Statement

Recently in-vivo liver decellularization has been considered as a promising approach to study in-vivo liver repopulation of a scaffold over ex-vivo. However, long term survival of in-vivo

liver decellularization has not yet been achieved. Here, despite anatomical and technical challenges, we successfully created a survival model of in-vivo selected liver lobe decellularization in rat, providing a major step towards in-vivo organ engineering.

Introduction

Recently, decellularization using detergents has become an attractive technique widely used in studies of tissue engineering. This technique is applied to fabricate a biological non-immunogenic acellular matrix, which can be used for further generation of an engineered tissue or organ. The potential applications of decellularized matrix followed by recellularization have been demonstrated for a variety of tissues, including trachea [1, 2], esophagus [3], bladder [4, 5], blood vessel [6-8], skin [9] and cartilage [10] . However, only some *ex-vivo* engineered structural tissues e.g. cartilage [10], bladder [4] and skin [11] but not functional organs e.g. lungs, heart or livers, have already been clinically used to treat patients.

Liver engineering has been emerging as a research hot spot around the world owing to the increasing demand of transplantable grafts for patients who need liver transplantation. However, researchers mainly study ex-vivo liver engineering [12-17]. Most of the transplantation studies used acellular or repopulated scaffolds for heterotopic transplantation to assess biocompatibility respectively selected functional aspects [18-22]. However, neither biliary duct (BD) nor hepatic artery (HA) was orthotopically anastomosized to the recipient. The maximally reported observation time was limited to 72 hours only [23, 24]. By far, orthotopic transplantation of an ex-vivo repopulated full liver graft has not yet been reported. Long term function and transplantation of engineered organs are still a vision. Therefore, looking for an alternative methodology to ex-vivo for studying liver engineering is needful [25].

Besides ex-vivo liver engineering, in-vivo liver engineering may represent a promising strategy to study hepatic repopulation under physiological conditions. The advantages of *in-vivo* partial liver engineering compared to ex-vivo liver engineering are as follows: Firstly, in contrast to ex-vivo perfusion with artificial culture medium, the *in-vivo* repopulated partial liver scaffold can receive physiological blood perfusion maintaining the organ at the physiological temperature, ensuring the needed amount of oxygen and growth factors [25]. Secondly, BD and HA are naturally preserved, in contrast to implantation of ex-vivo engineered liver lobes without anastomosis of either BD or HA as reported by other authors [20, 23, 26]. Last and most importantly, the remaining normal liver lobes maintain hepatic function allowing long term survival [25]. Pan and colleagues tried *in-vivo* decellularization and recellularization of the right inferior lobe in rat. However, all experimental animals were sacrificed after only 6 hours of intraoperative observation time in their trial. They claimed that the short lifespan of the animals may be due to the injury caused by the detergent used [27]. Postoperative survival has not yet been reported by now.

Prior to in-vivo liver lobe engineering, survival after in-vivo perfusion decellularization of a selected liver lobe is a prerequisite. Three main challenges need to be addressed: (1) Owing to the complicated intrahepatic vascular anatomy, the first challenge is to properly isolate the selected liver lobe and generate a fluid circuit bypass only through the isolated lobe compromising portal perfusion or venous drainage of the non-selected liver lobes. (2) Since the maximal operation time for an in-vivo liver lobe perfusion should not exceed 5 h [25], the second challenge is to identify a time-efficient in-vivo decellularization protocol not exceeding 2 h. Doing so is the prerequisite for later reseeding and cell settlement which might take another 2 h, leading to a total procedure time of about 5 h for liver engineering. (3) To prevent intra-abdominal corrosive injury by the detergent, the third challenge is to cover all other organs and tissues and drain the waste fluid without any contamination of the abdominal cavity.

Therefore, to establish survival after in-vivo liver lobe perfusion decellularization, three critical subgoals need to be accomplished: one is to achieve perfusion of the targeted liver lobe without blocking the vena cava and the main PV for a long period. In our previous study, we already accomplished this goal [25]. Second is to limit the decellularization time to 2 h. Third is to prevent the animal from chemical injury owing to detergent contamination during in-vivo decellularization.

To limit the decellularization duration, identifying a proper protocol for in-vivo decellularization which allows maintaining scaffold structure and preserving matrix proteins is critical. Detergents frequently used for ex-vivo liver decellularization include Triton X-100, SDS, or Triton combined with SDS [12-18, 24, 28-30]. The concentration of the Triton X-100 solution used for organ perfusion ranges from 0.5% up to 3% and the SDS solution from 0.01% to 1% [15, 20, 31-35]. Similarly, the decellularization time also ranges from hours up to several weeks [14, 19, 34, 35, 39, 40]. The flow rate employed in the protocols ranges from 1 to 200ml/min, depending on the species [15, 16, 20, 36-38]. In our previous study on ex-vivo liver decellularization in rodent, we used 1% SDS followed by 1% Triton as detergents for ex-vivo liver lobe decellularization in mouse and obtained an intact extracellular matrix within only 3 h of perfusion period [21]. To minimize the in-vivo decellularization duration to not more than 2 h, here we tried to compare three decellularization protocols of using the combination of 1% SDS followed by 1% Triton X100，1% Triton X100 only and 1% SDS only, to identify the ideal in-vivo partial liver lobe perfusion decellularization protocol in rat.

To prevent chemical damage during in-vivo decellularization, looking for an efficient drainage method to prevent contamination of the abdominal organs with the detergent is also important. However, no report has been published about drainage optimization during in-vivo decellularization. Preventing detergent from leakage into the abdominal cavity resulting in damaging other organs is rather challenging due to the difficulty of isolating the uneven

surface of the abdominal cavity and other organs from the being decellularized lobe. Therefore, here we also tried to create a novel isolation and sufficient drainage method for in-vivo partial liver lobe decellularization.

In brief, in a previous study we achieved the establishment of selected liver lobe perfusion technique [25]. We here further compared three in-vivo liver lobe decellularization protocols and two drainage methods to identify the ideal partial liver decellularization protocol. The key steps for the procedure are illustrated in **Figure 1**.

Material and Methods

Animals

In total, 43 male Lewis rats (aged at 11-13 weeks) were used (**Table 1**). All protocols were approved by The Thüringer Landesamt für Verbraucherschutz, Thuringia, Germany (Reg.No: UKJ-17-031) and conform to European guidelines on Care and Use of Laboratory Animals.

Experimental Design

The experiment was performed in three steps: (1) Small modifications of selective perfusion technique to adjust it for in-vivo decellularization (n=3). (2) Identification of optimal protocol for in-vivo selective liver lobe decellularization and characterization of the scaffold quality (n=25). (3) Prevention of contamination to abdominal cavity caused by the detergent (n=12) and histological assessment after postoperative 12 h for confirmation of short term physiological perfusion (n=3).

Modification of selective perfusion technique to make it suitable for in-vivo decellularization

Prior to decellularization, the rats (n=3) underwent a surgical circuit bypass only through the LLL based on small modifications of the perfusion technique previously reported [25].

In contrast to the previous study, where a suture ligation was used, here the left PV was blocked with micro-clamps (**Fig 2A**). This facilitated the insertion of the 24 G needle-free catheter as a fluid inlet. Using a second clamp, the left HA and the left BD as well as the left median PV, the left median HA and the left median BD were blocked. To speed up the procedure, we created the outlet (**Fig 2B**) in the left lateral HV by performing a small 1 mm long incision instead of using a catheter. Doing so facilitated the placement of the PDVC film and the dry gauze needed to protect the abdominal organs from the corrosive detergent solution during later in-vivo liver lobe decellularization. At the same time, detergent leaking from the surface of the organ could be absorbed. As a next step, selective perfusion of the LLL was started using 15 ml of heparinized saline (40 U/ml) at flow rate of 1 ml/min. Success of selective perfusion was judged based on the selective color change of LLL from fresh red to faint yellow as well as on a representative histological assessment, as reported before.

Comparison of three detergents for in-vivo perfusion decellularization

To identify the optimal protocol for in-vivo perfusion decellularization of the targeted LLL, we designed three experimental groups (n=6/group) for histological work-up. After heparin perfusion of the lobes using the modified perfusion technique, we compared perfusion of 1%SDS for 1 h followed by 1 h of 1%Triton with perfusion of either 2 h of only 1%Triton X or 2 h of only 1%SDS respectively.

Detergents were applied using a peristaltic pump (Harvard apparatus 70P, USA) (**Fig. 3A**), at a flow rate of 1.4 ml/min, 4 s interval, 1.8 ml/min for 2 hours. The abdominal cavity was protected from the contaminating detergent by covering all organs with PVDC film (**Fig. 3B**). Outflowing waste perfused fluid was drained using dry gauze (**Fig. 3C**).

Immediately after in-vivo perfusion decellularization, rats were sacrificed for assessment of decellularization efficiency based on macroscopic appearance of the liver lobe, histological assessment and DNA content.

The most efficient decellularization protocol was used for further characterization of scaffold quality. Integrity of the portal vascular tree was examined using injection of blue silicone rubber compound via the left PV followed by micro-CT scanning (n=3 scaffolds, and additional one normal as control). Integrity of the matrix structure of vascular and biliary tree and the sinusoidal network was assessed by histomorphology. The ultrastructure was visualized using scanning electron microscopy (n=2 scaffolds, and additional one normal as control). Preservation of matrix proteins (elastin, fibronectin, laminin, and collagen IV) was assessed based on immunohistochemical staining.

Comparison of two drainage methods to eliminate waste fluid during in-vivo perfusion decellularization

To prevent the abdominal organs from direct contact with the detergent leading to corrosive injury**,** we further designed another two groups (n=6/group) based on two different drainage methods: PVDC film + dry gauze and PVDC film + dry gauze + aspiration tube. For the first group, the drainage method of using PVDC film + dry gauze was performed as described in the first experiment. For the second group, an aspiration tube (**Fig. 3D**) was placed close to the base of the LLL for further drainage. After having put everything in place, the lobe was decellularized using the most efficient decellularization protocol determined before. Constant liver perfusion was achieved by the Harvard peristaltic pump at the same flow rate and duration as mentioned above. Detergent leakage, drainage efficiency and especially one week survival rate were taken as indicators of the optimal drainage method for in-vivo perfusion decellularization.

Physiological blood reperfusion of the decellularized scaffold in-vivo

After in-vivo perfusion decellularization of the LLL with the optimal detergent, the decellularized scaffold was flushed with 0.9% sodium chloride solution at a flow rate of 5ml/min for 10 min to remove most of the residual SDS from the approximately 3 ml scaffold. The incisions of the left PV and left lateral hepatic vein were closed with 11-0 prolene sutures. All micro-clamps were taken off the vessels to allow physiological blood reperfusion of the decellularized lobe. Macroscopic change of the color of the scaffold from transparent to bright red was taken as an indicator to confirm the success of in-vivo physiological reperfusion. The abdominal cavity was washed with 50 ml warm 0.9% sodium chloride solution to remove any possible contaminating SDS leaking from the liver lobe during decellularization. After closing the abdominal cavity, all rats in both groups were allowed to recover from anesthesia. Buprenorphine was administered subcutaneously in a dose of 0.05 mg/kg twice per day, so as to relieve postoperative pain. Totally, 6 rats per drainage group were used for one week survival analysis. With the most efficient drainage method determined from the above two groups, histological assessment at 12 hours postoperatively was performed to confirm the physiological reperfusion of the decellularized scaffolds (additional 3 rats).

Histological staining

Liver sections of 3 μm thickness were cut after formalin fixation and paraffin embedding. Sections were stained with histochemical dyes for haematoxylin and eosin staining. The stained sections were scanned at x 40 magnification with the scanner NanoZoomer 2.0 HT using the software NDP scan (Hamamatsu, Japan)

Verhoeff-Van Gieson staining (EvG staining)

Histological sections were dewaxed at 59 ºC in a warming cabinet for 30 min and then dehydrated through a descending alcohol series including Xylol and Alcohol (100%, 96% and

70%). The sections were rinsed with distilled water 3 times, followed by incubation with resorcinafuchsin (00088663, Hollborn&Söhne) 120 min. Afterwards they were rinsed with 96% alcohol until no more color clouds left, and again briefly washed with distilled water for 3 times. Mayer´s hematoxylin (T865.3, Roth) was applied to stain the sections for 30 min. After being washed with distilled water 3 times, the sections were further stained with Van Gieson (Ch.-B.:0219, Apotheke) They were again washed with distilled water and dehydrated through an ascending alcohol series including alcohol (70%, 96% and 100%) and Xylol, and then coverslipped. The stained sections were scanned in the same way as described above. (Nuclei, black brown; Cytoplasm, light brown; Collagen, red).

Digitalized images were used for the morphological analysis. First, we checked the H&E images from the scaffolds subjected to different decellularization protocols for the presence of remaining liver cells or cellular debris (nuclei, purple/black). Second, structural integrity (collagen, pink) was also assessed based on the H&E staining of scaffolds obtained after 1% SDS-only decellularization. We identified the key features of the hepatic acinus such as the portal field with the PV, HA and the BD as well as the CV based on the appearance of the matrix structure (collagen, pink). We than assessed the integrity of the sinusoidal matrix structure based on the continuity of the network. We further judged the optimal decellularization protocol based on EvG staining.

Immunohistochemical staining

To further assess matrix proteins of the scaffold, immunostaining was performed. Briefly, sample tissues were fixed 4% formaldehyde and then embedded with paraffin. Liver sections were cut into 3 μm thickness. A panel of primary rabbit antibodies were used for immunostaining: Anti-collagen IV (ab6586, 1:500, abcam), Anti-fibronectin (ab2413, 1:200, abcam), Anti-elastin (ab21610, 1:100, abcam) and Anti-laminin (ab11575, 1:1000, abcam). Following three washes with TBST, the samples were stained according to the manual of

EnVision ® + System-HRP Labelled Polymer Anti-Rabbit (K4011, Dako). Thereafter the sample was counterstained with hematoxylin for 7 min, and then rinsed with tap water for 10 min. After dehydration with ethanol (70%, 96%, and 100%) and xylol in sequence, the samples were mounted with mounting medium (41-4011, Medite) before imaging.

Preservation of the main extracellular matrix proteins in the portal field and the sinusoidal network was assessed by comparing immunohistochemical images from normal and decellularized liver samples.

Silicon rubber compound staining

To visualize the integrity and patency of the portal vascular tree, 0,5 ml blue silicone rubber injection contrast agent (MV120, MICROFIL®, USA) was administered via the left PV in normal and decellularized LLLs. About 20 min after injection, the compound polymerized. Integrity of the portal tree of the scaffold was judged based on the continuous contrasting of vascular tree as well as the detection of intrahepatic leakage.

Micro-CT scanning

The scaffold injected with silicone rubber compound was explanted and stored in formalin solution at 4 degree for over 48 hours for fixation. For µCT scanning of the scaffold, the liver sample was taken out of the fixation solution and placed onto a µCT bed. Then the bed with scaffold was put into the µCT machine. A high resolution µCT (SkyScan1272, Bruker, Billerica, MA, USA) acquired 940 projections with 2688 x 4032 pixels with 3186 ms exposure time, with total duration of 8 hours. The x-ray tube was operated at voltage 60 kV and current 0.166 mA with an aluminum filter of 0.25 mm thickness. After scanning, a volumetric stack with voxel size 6.6 µm was constructed by filtered backprojection. The images were used for 3D-reconstrution of the portal tree using the software IMALYTICS Preclinical 2.0 [42].

To assess the structural integrity of the portal tree, we determined the continuity of the vascular tree after 3D-reconstruction and the level of branching.

Scanning electron microscopy

To evaluate the three-dimensional ultrastructure of the decellularized scaffold, scanning electron microscopy was conducted. A normal and a decellularized LLL were subjected to perfusion fixation with 20 ml of a mixture of 4% paraformaldehyde, 2.5% glutaraldehyde and 0.1 M cacodylate buffer (pH 7.4). After perfusion, the LLL was excised and placed into the fixative for 24h at room temperature. Afterwards the samples were washed three times for 10 minutes each with cacodylate buffer and dehydrated in ascending ethanol concentrations (30, 50, 70, 90 and 100%) for 10 minutes each. Subsequently, the samples were critical-point dried using liquid CO_2 and sputter coated with gold (thickness approx. 4 nm) using a SCD005 sputter coater (BAL-TEC, Liechtenstein) to avoid surface charging. Finally the specimens were investigated with a field emission (FE) SEM LEO-1530 Gemini (Carl Zeiss NTS GmbH, Oberkochen, Germany.

Images were taken at different magnifications. Similar to the histological investigation we focused on determining the integrity of the ultrastructure of the matrix in the portal triad and of the CV. We also assessed the integrity of the ultrastructure of the sinusoidal matrix network.

DNA quantification

To further assess the complete removal of cells in the decellularized scaffold, DNA quantification was carried out. DNA was extracted from a small piece (up to 25mg) of excised normal liver and the decellularized scaffolds using QIAamp DNA Mini Kit (QIAGEN) according to the instruction of QIAamp DNA Mini and Blood Mini Handbook (2016, QIAGEN). DNA-concentration was measured by Spectrophotometry using a Nanodrop1000.

Statistical Analysis

All results are presented as mean ± standard deviation. Statistical comparisons were made through the use of a Student's t-test performed within SPSS Statistics 25. Statistical significance was determined to be $p < 0.05$.

Results

Selective perfusion of the left lateral lobe using the modified method

After perfusion of the LLL with heparinized saline, the lobe did gradually change the color from red to faint yellow (**Fig 4A-B**), indicating that the blood in the portal system of the lobe was completely washed out. However, as reported before, clamping of the left lateral PV caused ischemia of the left median lobe (**Fig 4B**). The histological assessment of the lobe further confirmed that no blood cells were visible in the PV branches and CVs, compared to a native liver lobe (**Fig 4C-F**). This indicates that the modified in-vivo circuit bypass also enabled the selective perfusion of the LLL without causing any further damage.

Identification of the optimal decellularization protocol for in-vivo perfusion decellularization

Using **1% Triton X100 followed by 1% SDS** within 2 hours resulted in incomplete removal of the cellular components of the liver lobe as indicated by non-translucent areas of different size (**Fig. 5A-D**). Histology revealed large areas of cell-free parenchyma interspersed with islands of remaining cells, confirming the incomplete decellularization result (**Fig. 6B**). Correspondingly, the DNA concentration after random sampling of the liver was as high as 1366.92± 500.89 ng/mg (n= 6/6, wet tissue), which is about 50% of the normal liver (3091.31± 192.89 ng/mg, n=6/6) ($P < 0.0001$).

Perfusion with **1% TritonX100** alone did not result in decellularization but caused a smooth change in color from faint yellow to a non-translucent white appearance of the LLL within 2 h (**Fig. 5E-H**). Similarly histology showed that hepatic parenchyma was not removed. However, detergent perfusion caused the loss of nuclear stain in the majority of the liver cells, suggesting at least severe damage or death of the cells. Interestingly a small rim of seemingly vital cells was seen in the vicinity of the portal field. In between the hepatic chords large empty spaces became visible suggesting the removal of at least some hepatocytes (**Fig. 6C**). These finding were confirmed by the DNA-concentration measurement revealing slightly lower levels (2614.94±547.73 ng/mg, n=6/6) ($P=0.16 > 0.01$) than in the normal liver.

In contrast, perfusion with **1% SDS** alone gradually cleared the liver from all cellular components within 2 h as indicated by the translucent appearance (**Fig. 5I-L**). No areas with remaining cells or cellular debris were detected in any of the histological sections (**Fig. 6D**). Correspondingly, the remnant DNA concentration was as low as 57.40±11.71 ng/mg, which represents less than 2% of the DNA-concentration of normal liver lobe ($P< 0.00001$) (**Fig.7**).

Taken together, these findings suggest that in-vivo decellularization with 1% SDS only for 2 h is very effective compared to the other two protocols and was therefore used in the subsequent experiments.

Characterization of the scaffolds generated with the optimal decellularization protocol (1%SDS)

First we characterized the vascular tree of the scaffold generated with the optimal decellularization protocol based on macroscopic evaluation. The vascular trees including the PV tree system and HV system (**Fig. 8A**) are macroscopically visible in the translucent matrix. The blue silicon rubber compound solution injected through the left PV appeared as expected inside the portal vascular network. Upon injection, it gradually moved from the lobar portal

vein vessels to smaller venules, indicating the integrity of the portal vascular structure (**Fig. 8B**). Since injection was stopped when the blue compound reached the finest branches of the portal vascular tree, the hepatic venous tree appeared white in the otherwise translucent scaffold (**Fig. 8B**).

We further visualized the portal vascular tree in three dimensions by Micro-CT scanning and 3D reconstruction. CT scanning confirmed that the continuity of portal vascular tree was clearly visible upon 3D reconstruction. Furthermore, the large sized lobar portal vessels up to the forth to fifth order (**Fig. 8D**) remained intact, which is comparable to the normal LLL.

Second, histological staining of the scaffold showed key features of the hepatic acinus. Portal fields could be clearly identified based on remaining matrix structure of PV, HA and BD. CVs appeared as single vascular matrix structures. In addition, the decellularized hepatic lobules appeared as dense network of sinusoidal structures resembling a spider net (**Fig.6D**). These findings suggest that hepatic microarchitecture was morphologically preserved after in-vivo decellularization of the selected liver lobe.

Third, the scanning electron microscopy images revealed the integrity of the ultra- structure of the matrix including the PV, HA, BD (**Fig.8F**) and the CV (**Fig.8G**). We observed the continuous sinusoidal matrix network in the parenchyma of the scaffold (**Fig.8F-G**). These findings show the integrity of the ultravascular structure in the decellularized liver scaffold, compared to native liver lobe.

As the forth and last step, using a staining panel consisting of histochemical and immunohistochemical methods, the protein components of the scaffold were assessed.

Using the **EVG-staining**, we observed strong red signals (collagen) in the portal field (**Fig.9 A-B**) and around the CV (**Fig.9 C-D**) of the scaffold, similar as in the native liver. Compared to the portal field, the staining intensity in the sinusoidal matrix network was much weaker,

indicative of the different collagen content in the structures. In the scaffold, we did neither observe any black nuclear signals, nor any yellowish cytoplasmic stain, indicating the removal of cells or cell remnants. As expected, we saw only a faint dark purple signal in the HA of the native liver but not clearly in the scaffold.

This was further confirmed by the **Collagen IV**-staining. We observed an over-all stronger signal in both the native liver and the decellularized scaffold. The strong signal in the portal field, especially in the basal membranes, facilitated the identification and differentiation of the three key structures PV, HA and BD (**Fig.9 E-F**). Due to the strong staining of the basal membrane also the CV (**Fig.9 G-H**) could be detected easily. Furthermore, the strong staining of the sinusoidal network can be taken as indicator of the preservation of the sinusoidal matrix.

The immunohistochemical signal for **Laminin**, normally expressed in the basal membrane of vessels and to a much lesser extent also in the sinusoids, was strong in the portal field (**Fig.9 I-J**) and in the CV (**Fig.9 K-L**). In contrast, the signal was rather weak in the sinusoidal network, also reflecting the preservation of the physiological distribution of the ECM-protein.

Fibronectin is one of the most abundant proteins in the perisinusoidal space surrounding the periportal and CV regions [43]. We observed a strong signal in the portal field (**Fig.9 M-N**) and around the CV (**Fig.9 O-P**) of the native liver, which was less pronounced in the scaffold. Similarly, we observed a slightly weaker signal in the sinusoidal matrix of the scaffold compared to the native liver. This gives rise to the speculation, that the detergent might have affected the fibronectin content of the scaffold.

Elastin is mainly expressed in the vasculature of normal liver as indicated by strong brown signals but less in the sinusoids, as visualized by light brown signals **(Fig.9 Q and S)**. In the LLL scaffold, strong signal intensity was seen in the portal field **(Fig.9 R)** and in the CV

(Fig.9 T), which is similar to the pattern observed in normal liver. Similarly, the staining intensity was much fainter in the sinusoidal network, both suggesting preservation of this ECM-protein as well.

Identification of the optimal organ protection during in-vivo decellularization (1%SDS)

During in-vivo perfusion decellularization, waste fluid emerged from the incision hole in the left lateral HV but also from the surface of the liver (**Fig.10**), in total about 200 ml within the 2 h procedure. To protect the abdominal cavity and all organs completely from this volume, placement of the PVDC film covered by gauzes was insufficient to absorb and drain this large amount of corrosive waste fluid. Animals subjected to this procedure died within 48 hours (n=5/6) and just only one (n=1/6) survived for at less one week. Only after placing an additional suction tube between the gauze layers, complete prevention of contamination was achieved. All animals (n=6/6) subjected to the drainage method of PVDC film + dry gauze + suction tube tolerated the procedure well as indicated by the survival rate of 100% after the 7 d observation time. In contrast in the group of rats subjected to the simple procedure (no suction tube), only 16.7% (1/6) reached the end of the observation period, as shown in the Kaplan-Meier curve (**Fig.11**). None of the rats subjected to the combination of PVDC film + dry gauze + suction tube suffered from any severe postoperative complications. The maximal body weight loss during the first 7 post-op days was less than 20% and occurred on postoperative day 2-3, and with a fast recovery thereafter (**Fig.12**). This observation suggests that the procedure was well tolerated and that did not experience severe toxic SDS-related side effects.

Physiological reperfusion of the decellularized scaffold in-vivo

After closing the incision on the left PV and the left lateral HV and reopening the blocked left PV, artery and BD to the left lateral scaffold, the color of the scaffold changed back from translucent (**Fig.13A**) into red (**Fig.13C**), suggesting blood reperfusion of the scaffold.

Histology obtained 12 h after reperfusion revealed large amounts of erythrocytes in PV, sinusoidal network and CV, albeit distributed very inhomogeneously throughout the section. In all 3 animals we also found blood clots in large intralobar vessels leading to a partial blockade of the vessel (**Fig.13D-E**). Furthermore, in one of the 3 animals we observed an alteration of erythrocytes and formation of hemoglobin crystals in some areas of the section (**Fig.13F**).

Discussions

In this study we demonstrate for the first time long-time survival after in-vivo liver lobe decellularization and physiological reperfusion in rats. Furthermore, our technique resulted in remarkable scaffold quality.

Decellularization time

In comparison to the first report of in vivo decellularization by Pan [27], our procedure took longer with 2 h compared to 1 h reported by them. This might be related to the size of the targeted liver lobe with the LLL being 5-fold the size of the right superior liver lobe, according to the rat liver volume measurement reported by Madrahimov [43]. Nevertheless, completing the operation including laparotomy, decellularization and closure within 3 h still allows using up to 90 min for reseeding the organ in-vivo to keep the total time below 5 h. Our previous study investigating in-vivo perfusion of the LLL revealed that an operation time of less than 5 hours was still tolerated by the animals. However, when prolonging the time to

5 hours or more, the rats developed transient diarrhea and bloody ocular discharge [25]. In contrast, Pan needed about 2 hours for in-vivo decellularization and reseeding, but sacrificed the rats intraoperatively after additional 6 h of observation without even attempting to assess the survival rate and time.

Using 1% SDS for in-vivo liver lobe decellularization resulted in a complete removal of cells in the targeted liver lobe within 2 h, which is even more time-efficient than using Triton X100 alone or the sequential application of Triton X and SDS in our study. Additionally, loss and destruction of matrix protein might be related to the exposure time to the harsh detergents, as shown in detail for porcine aorta by Guler [44]. Therefore, it is critical to reduce the exposure time for the sake of preserving more matrix proteins. Using only 2 hours of 1% SDS-perfusion for in-vivo decellularization is substantially shorter compared to the duration of ex-vivo decellularization ranging from hours to days or even weeks reported by other authors mentioned above. The reason why we could shorten the decellularization time may be due to an extensive heparin saline flush of the live lobe prior to decellularization. Using heparin did not only help to prevent disseminated intravascular coagulation but also dissolved small thrombi formed in the vessel after clamping. Such microthrombi causing obstruction may hinder the flow of the detergent into the liver lobe and slow down the process of decellularization.

Decellularized scaffold quality

Our work suggests that in-vivo selective liver lobe decellularization did create a translucent liver matrix while preserving the integrity of the matrix structure. PV, HA, BD and CV, as well as the ultrastructure of the matrix were confirmed by CT, histology and SEM. The main matrix proteins including laminin, elastin, fibronectin and collagen IV were preserved as indicated by the presence of strong signals in immunohistochemistry. Therefore, we could apparently identify and discriminate all vascular structures in the portal field and visualized

the continuous sinusoidal network using standard immunohistochemical staining. We provide the first data of a very detailed description of the fine structures of in-vivo decellularized liver lobe scaffolds in contrast to other reports, which just claimed their structural integrity based on a global assessment [16, 24, 35, 45].

SDS contamination and toxicity

Since long term survival is the prerequisite for establishing in-vivo liver engineering successfully, this was the reason why we solved the drainage problem first before focusing on scaffold repopulation. Detergent waste fluid emerged not only from the incision in left lateral HV, but also from the whole surface of the targeted liver lobe during in-vivo perfusion decellularization process. Therefore, the whole abdominal cavity and all abdominal organs were at risk of contamination with the detergent. Pan and co-workers [27] already identified the risk of contamination, but only used a catheter placed in the outlet created in the inferior vena cava (IVC). This catheter can effectively drain a substantial amount of the waste fluid, however cannot prevent contamination with waste fluid emerging from the surface of the liver lobe undergoing decellularization.

We efficiently prevented the outflowing detergent waste fluid from contaminating non-targeted tissue and organs in the abdominal cavity by covering them with PVDC film. PVDC film is widely used for wrapping food [46, 47] because it is insoluble in oil and organic solvents. It has a very low moisture regain and is impervious to mold and bacteria. PVDC seems to act as a remarkable barrier not only against water, oxygen, and aromas but also against base and acid solutions. Besides using the mechanical PVDC barrier, we efficiently drained the waste fluid using dry gauze as well as an aspiration tube. Reduction of contamination by using an aspiration tube in addition to the PVDC-film and dry gauze seemed to be most decisive for the survival of the animals.

Furthermore, we did not only perfuse the decellularized scaffold with warm saline solution, but also flushed the abdominal cavity with warm saline solution after decellularization to wash away the residual SDS.

Thereby, all these measures together enabled the long term survival of the animals without experiencing severe toxic side effects. Additionally, the maximal postoperative body weight loss never exceeded 20% and recovered from postoperative day 3 onwards. Based on our observations we concluded that using the combination of PVDC film + dry gauze + aspiration tube as drainage method together with a though perfusion of the scaffold and a wash of the scaffold and the abdominal cavity resulted in an efficient prevention of a potential contamination with residual SDS. Therefore, we did not go deeper in the exploration of potential systemic toxic effects of the SDS.

Limitations

Despite of anatomical and technical challenges, we successfully established a survival model of in-vivo selective liver lobe decellularization rat. However, there are also some limitations: First, since the left PV supplies the left lateral PV and the left lateral PV, transient ischemia of the left median lobe (only representing approx.15% of the whole liver in volume) is inevitable due to blockage of the left PV. Transient ischemia might induce some liver damage, but is not putting the animal at a vital risk.

Furthermore, other rarely used detergents like deoxyribonuclease (DNase) [48, 49], sodium lauryl ether sulfate (SLES) [48] and sodium deoxycholate (NaDOC) [50], possibly resulting in an even shorter time for in-vivo decellularization were not included in the comparison of the decellularization protocols.

Finally, the “naked” collagen of the scaffold can activate the extrinsic coagulation system upon contact with blood upon reperfusion. Therefore, it is not surprising that we observed

blood clots in the scaffold similar as also reported by others [23, 26, 27]. This might explain the very inhomogeneous distribution of blood cells within the scaffold. Another interesting finding was the observation of altered swollen erythrocytes and the formation of crystals which were also distributed inhomogeneously throughout the scaffold. Both together, swollen erythrocytes potentially undergoing hemolysis and releasing hemoglobin in direct neighborhood to crystals lead to the suspicion that hemoglobin crystals did form. Hemoglobin crystal formation was observed previously, in the brain of rats with experimental intracerebral hemorrhage [51], in lungs with pulmonary hemorrhage of varying etiologies [52-54], but also as a result of pressure injury to rat dentition [55]. In our case, hemoglobin crystal formation might be due to toxic injury because of minimal residual SDS trapped in the protein structure of the scaffold leading to hemolysis with subsequent release of hemoglobin. Assuming a volume of the LLL of approximately 3 ml, we perfused the lobe with 50 ml saline solution, 17-fold higher volume which should lead to substantial reduction of remaining SDS. However, it cannot be excluded that even low levels of SDS binding to the scaffold proteins might cause local hemolysis with subsequent crystal formation.

Furthermore, it is highly likely that the loss of cells reduces the stability of the resulting scaffold rendering the scaffold very prone to perfusion inhomogeneities. Inhomogeneous perfusion may result in an incomplete wash and a highly variable distribution of blood reperfusion resulting in locally different levels of residual SDS as indicated by an inhomogeneous distribution of hemoglobin crystals.

Perspective

Both observations of clot formation and haemoglobin crystallization call for a kinetic observation of the reperfusion process over time to investigate the reperfusion quality of the scaffold and the effectivity of the wash-out procedure. For excluding any potential local and systemic toxicity of residual SDS, a number of tests could be performed at different

observation time points during the first postoperative week such as (1) a detailed histologic work-up of the scaffold to better understand the timing of blood clot and crystal formation, (2) blood count to detect any eventual hemolysis, (3) determination of local SDS-scaffold and systemic SDS-blood levels as direct evidences of SDS contamination, histology of other organs e.g. heart, lung, kidney, spleen and undecellularized liver lobes, as well as (4) clinical chemistry including liver function and renal function to identify any organ-specific effect.

Since blood clots were observed in the blood reperfused scaffold, we believe that the next urgent problem to address is to prevent coagulation in the scaffold for ensuring in-vivo physiological perfusion. It is highly unlikely that reseeding the scaffold with endothelial cells with a very short time for cell adherence is sufficient to prevent clotting. Recently one interesting technique was suggested by Bruinsma [56] for preventing coagulation when transplanting a repopulated liver scaffold. They reported applying a layer-by-layer heparin coating technique to a scaffold before reseeding the scaffold in-vitro prevented coagulation.

Once anticoagulation in-vivo is achieved, we will pursue in-vivo liver reengineering by in-vivo recellularization of the liver scaffold with hepatocytes and non-parenchymal cells, as done ex-vivo by other authors [23, 24, 56-59].

For fundamental research, the key benefit of in-vivo partial liver decellularization is its potential for promoting the understanding of liver engineering by in-vivo repopulation of a liver scaffold.

Clinical applicability is hampered by the difference in the lobar and vascular anatomy of the liver. The human liver represents one large organ which is separated by the underlying vasculature in a right and left lobe, but without being separated into two anatomically distinct lobes. Therefore creating a bypass circuit is only possible after parenchymal transection as performed in the ALPPS-procedure (Associating Liver Partition & Portal Vein Ligation for

Staged Hepatectomy) [60]. This is a therapeutic surgical procedure which is currently used to enhance resectability for otherwise unresectable liver tumors by ligating the portal vein from one liver lobe to promote regeneration of the other partitioned liver lobe. Therefore, in-vivo selective lobe perfusion followed by decellularization would be feasible after parenchymal transection. In-vivo selective liver lobe decellularization may be an alternative method of chemical resection for patients with diseased livers, e.g., lobular liver cancer [25, 27] or various hepatic-based metabolic disorders. And then hepatic function could be restored through in-vivo repopulation of the decellularized scaffold with healthy liver cells or stem cells [27]. In most hepatic metabolic disorders, recovery of only about 10% of the original enzyme activity is sufficient to ensure adequate metabolic control [61-62].

Conclusions

Overall, despite of technical and anatomic challenges, we provide the first data on having successfully established a survival model of in-vivo partial liver decellularization in living rats, which represents groundwork towards in-vivo organ engineering.

Competing interest statement

There is no conflict of interest. The two copyrighted images in Figure 1 were reused from Wang and permitted by the JoVE.

Acknowledgements

This project is funded by Chinese scholarship Council (Fund Number: CSC NO: 2017080801619). Special thanks go to Jens Geiling from the Institute of Anatomy I, Jena University Hospital for producing the schematic drawings of rat liver anatomy.

References

1. MacChiarini, P., et al., *First human transplantation of a bioengineered airway tissue.* The Journal of Thoracic and Cardiovascular Surgery, 2004. **128**(4): p. 638-641.
2. Macchiarini, P., et al., *Clinical transplantation of a tissue-engineered airway.* The Lancet, 2008. **372**(9655): p. 2023-2030.
3. Nieponice, A., T.W. Gilbert, and S.F. Badylak, *Reinforcement of esophageal anastomoses with an extracellular matrix scaffold in a canine model.* Ann Thorac Surg, 2006. **82**(6): p. 2050-8.
4. Atala, A., et al., *Tissue-engineered autologous bladders for patients needing cystoplasty.* The Lancet, 2006. **367**(9518): p. 1241-1246.
5. Yoo, J.J., et al., *Bladder augmentation using allogenic bladder submucosa seeded with cells.* Urology, 1998. **51**(2): p. 221-5.
6. L'Heureux, N., T.N. McAllister, and L.M. de la Fuente, *Tissue-engineered blood vessel for adult arterial revascularization.* N Engl J Med, 2007. **357**(14): p. 1451-3.
7. Shin'oka, T., Y. Imai, and Y. Ikada, *Transplantation of a tissue-engineered pulmonary artery.* N Engl J Med, 2001. **344**(7): p. 532-3.
8. Dahl, S.L., et al., *Decellularized native and engineered arterial scaffolds for transplantation.* Cell Transplant, 2003. **12**(6): p. 659-66.
9. Schechner, J.S., et al., *Engraftment of a vascularized human skin equivalent.* Faseb j, 2003. **17**(15): p. 2250-6.

10. Mumme, M., et al., *Nasal chondrocyte-based engineered autologous cartilage tissue for repair of articular cartilage defects: an observational first-in-human trial.* Lancet, 2016. **388**(10055): p. 1985-1994.

11. Kirsner, R.S., V. Falanga, and W.H. Eaglstein, *The development of bioengineered skin.* Trends Biotechnol, 1998. **16**(6): p. 246-9.

12. Cheng, Y., et al., *In vitro culture of tumour-derived hepatocytes in decellularised whole-liver biological scaffolds.* Digestion, 2013. **87**(3): p. 189-95.

13. Pan, M.X., et al., *An efficient method for decellularization of the rat liver.* J Formos Med Assoc, 2014. **113**(10): p. 680-7.

14. Struecker, B., et al., *Improved rat liver decellularization by arterial perfusion under oscillating pressure conditions.* J Tissue Eng Regen Med, 2014.

15. Baptista, P.M., et al., *The use of whole organ decellularization for the generation of a vascularized liver organoid.* Hepatology, 2011. **53**(2): p. 604-17.

16. Yagi, H., et al., *Human-scale whole-organ bioengineering for liver transplantation: a regenerative medicine approach.* Cell Transplant, 2013. **22**(2): p. 231-42.

17. Nari, G.A., et al., *Preparation of a three-dimensional extracellular matrix by decellularization of rabbit livers.* Rev Esp Enferm Dig, 2013. **105**(3): p. 138-43.

18. Badylak, S.F., D. Taylor, and K. Uygun, *Whole-organ tissue engineering: decellularization and recellularization of three-dimensional matrix scaffolds.* Annu Rev Biomed Eng, 2011. **13**: p. 27-53.

19. Mazza, G., et al., *Decellularized human liver as a natural 3D-scaffold for liver bioengineering and transplantation.* Sci Rep, 2015. **5**: p. 13079.

20. Jiang, W.C., et al., *Cryo-chemical decellularization of the whole liver for mesenchymal stem cells-based functional hepatic tissue engineering.* Biomaterials, 2014. **35**(11): p. 3607-17.

21. Mussbach, F., et al., *Bioengineered Livers: A New Tool for Drug Testing and a Promising Solution to Meet the Growing Demand for Donor Organs.* Eur Surg Res, 2016. **57**(3-4): p. 224-239.

22. Mussbach, F., et al., *[Liver engineering as a new source of donor organs : A systematic review]*. Chirurg, 2016. **87**(6): p. 504-13.

23. Bao, J., et al., *Construction of a portal implantable functional tissue-engineered liver using perfusion-decellularized matrix and hepatocytes in rats.* Cell Transplant, 2011. **20**(5): p. 753-66.

24. Uygun, B.E., et al., *Organ reengineering through development of a transplantable recellularized liver graft using decellularized liver matrix.* Nat Med, 2010. **16**(7): p. 814-20.

25. Au - Wang, A., et al., *A Novel Surgical Technique As a Foundation for In Vivo Partial Liver Engineering in Rat.* JoVE, 2018(140): p. e57991.

26. Kojima, H., et al., *Establishment of practical recellularized liver graft for blood perfusion using primary rat hepatocytes and liver sinusoidal endothelial cells.* Am J Transplant, 2018. **18**(6): p. 1351-1359.

27. Pan, J., et al., *In-vivo organ engineering: Perfusion of hepatocytes in a single liver lobe scaffold of living rats.* Int J Biochem Cell Biol, 2016. **80**: p. 124-131.

28. Uygun, B.E., et al., *Decellularization and recellularization of whole livers.* J Vis Exp, 2011(48).

29 De Kock, J., et al., *Simple and quick method for whole-liver decellularization: a novel in vitro three-dimensional bioengineering tool?* Arch Toxicol, 2011. **85**(6): p. 607-12.

30. Kang, Y.Z., Y. Wang, and Y. Gao, *[Decellularization technology application in whole liver reconstruct biological scaffold]*. Zhonghua Yi Xue Za Zhi, 2009. **89**(16): p. 1135-8.

31. Soto-Gutierrez, A., et al., *A whole-organ regenerative medicine approach for liver replacement.* Tissue Eng Part C Methods, 2011. **17**(6): p. 677-86.

32. Lee, J.S., et al., *Liver extracellular matrix providing dual functions of two-dimensional substrate coating and three-dimensional injectable hydrogel platform for liver tissue engineering.* Biomacromolecules, 2014. **15**(1): p. 206-18.

33. Baptista, P.M., et al., *Whole organ decellularization - a tool for bioscaffold fabrication and organ bioengineering.* Conf Proc IEEE Eng Med Biol Soc, 2009. **2009**: p. 6526-9.

34. Mattei, G., et al., *Mechanostructure and composition of highly reproducible decellularized liver matrices.* Acta Biomater, 2014. **10**(2): p. 875-82.

35. Barakat, O., et al., *Use of decellularized porcine liver for engineering humanized liver organ.* J Surg Res, 2012. **173**(1): p. e11-25.

36. Geerts, S., et al., *Nondestructive Methods for Monitoring Cell Removal During Rat Liver Decellularization.* Tissue Eng Part C Methods, 2016. **22**(7): p. 671-8.

37. Wu, Q., et al., *Optimizing perfusion-decellularization methods of porcine livers for clinical-scale whole-organ bioengineering.* Biomed Res Int, 2015. **2015**: p. 785474.

38. Ren, H., et al., *Evaluation of two decellularization methods in the development of a whole-organ decellularized rat liver scaffold.* Liver Int, 2013. **33**(3): p. 448-58.

39. Lang, R., et al., *Three-dimensional culture of hepatocytes on porcine liver tissue-derived extracellular matrix.* Biomaterials, 2011. **32**(29): p. 7042-52.

40. Buhler, N.E., et al., *Controlled processing of a full-sized porcine liver to a decellularized matrix in 24 h.* J Biosci Bioeng, 2015. **119**(5): p. 609-13.

41. Gremse, F., et al., *Imalytics Preclinical: Interactive Analysis of Biomedical Volume Data.* Theranostics, 2016. **6**(3): p. 328-41.

42. Kim, T.H., et al., *Extracellular matrix remodeling at the early stages of liver regeneration in the rat.* Hepatology, 1997. **26**(4): p. 896-904.

43. Madrahimov, N., et al., *Marginal hepatectomy in the rat: from anatomy to surgery.* Ann Surg, 2006. **244**(1): p. 89-98.

44. Guler, S., et al., *Improvement of Decellularization Efficiency of Porcine Aorta Using Dimethyl Sulfoxide as a Penetration Enhancer.* Artif Organs, 2018. **42**(2): p. 219-230.

45. White, L.J., et al., *The impact of detergents on the tissue decellularization process: A ToF-SIMS study.* Acta Biomater, 2017. **50**: p. 207-219.

46. G.Piringer, o., *Plastic Packaging: Interactoins with Food and Pharmaceuticals*. 2008: Weinheim.

47. Marsh, K. and B. Bugusu, *Food Packaging—Roles, Materials, and Environmental Issues.* Journal of Food Science, 2007. **72**(3): p. R39-R55.

48. Kawasaki, T., et al., *Novel detergent for whole organ tissue engineering.* J Biomed Mater Res A, 2015. **103**(10): p. 3364-73.

49. Shirakigawa, N., T. Takei, and H. Ijima, *Base structure consisting of an endothelialized vascular-tree network and hepatocytes for whole liver engineering.* J Biosci Bioeng, 2013. **116**(6): p. 740-5.

50. Wang, Y., et al., *Method for perfusion decellularization of porcine whole liver and kidney for use as a scaffold for clinical-scale bioengineering engrafts.* Xenotransplantation, 2015. **22**(1): p. 48-61.

51. Kleinig, T.J., et al., *Hemoglobin crystals: A pro-inflammatory potential confounder of rat experimental intracerebral hemorrhage.* Brain Research, 2009. **1287**: p. 164-172.

52. Ghio, A.J., et al., *Iron disequilibrium in the rat lung after instilled blood.* Chest, 2000. **118**(3): p. 814-23.

53. Paakko, P., et al., *Biochemical and morphological characterization of carbon tetrachloride-induced lung fibrosis in rats.* Arch Toxicol, 1996. **70**(9): p. 540-52.

54. Zachary, J.F., et al., *Temporal and spatial evaluation of lesion reparative responses following superthreshold exposure of rat lung to pulsed ultrasound.* Ultrasound Med Biol, 2001. **27**(6): p. 829-3

55. Rygh, P. and K.A. Selvig, *Erythrocyte crystallization in rat molar periodontium incident to tooth movement.* Scand J Dent Res, 1973. **81**(1): p. 62-73.

56. Bruinsma, B.G., et al., *Layer-by-layer heparinization of decellularized liver matrices to reduce thrombogenicity of tissue engineered grafts.* J Clin Transl Res, 2015. **1**(1).

57. Zheng, Y. and M.A. Roberts, *Scalable vascularized implants.* Nature Materials, 2016. **15**: p. 597.

58. Ko, I.K., et al., *Bioengineered transplantable porcine livers with re-endothelialized vasculature.* Biomaterials, 2015. **40**: p. 72-9.

69. Devalliere, J., et al., *Improving functional re-endothelialization of acellular liver scaffold using REDV cell-binding domain.* Acta Biomater, 2018. **78**: p. 151-164.

60. Li, J., et al., *Associating liver partition and portal vein ligation for staged hepatectomy: From technical evolution to oncological benefit.* World J Gastrointest Surg, 2016. **8**(2): p. 124-33.

61. Ban, K., et al., *A pediatric patient with classical citrullinemia who underwent living-related partial liver transplantation.* Transplantation, 2001. **71**(10): p. 1495-7.61.

62. Meyburg, J. and G.F. Hoffmann, *Liver transplantation for inborn errors of metabolism.* Transplantation, 2005. **80**(1 Suppl): p. S135-7.

Figures and legends

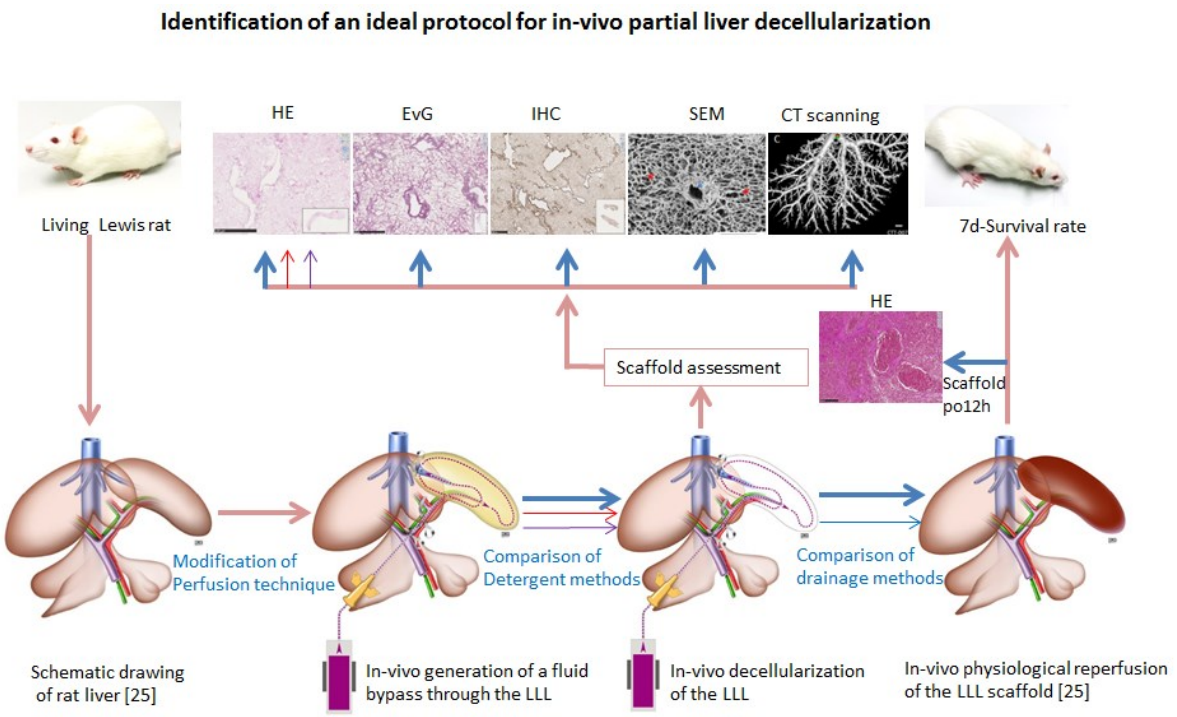

Figure 1.The scheme of identification of an ideal protocol for survival model of in-vivo partial liver lobe decellularization in live rat.

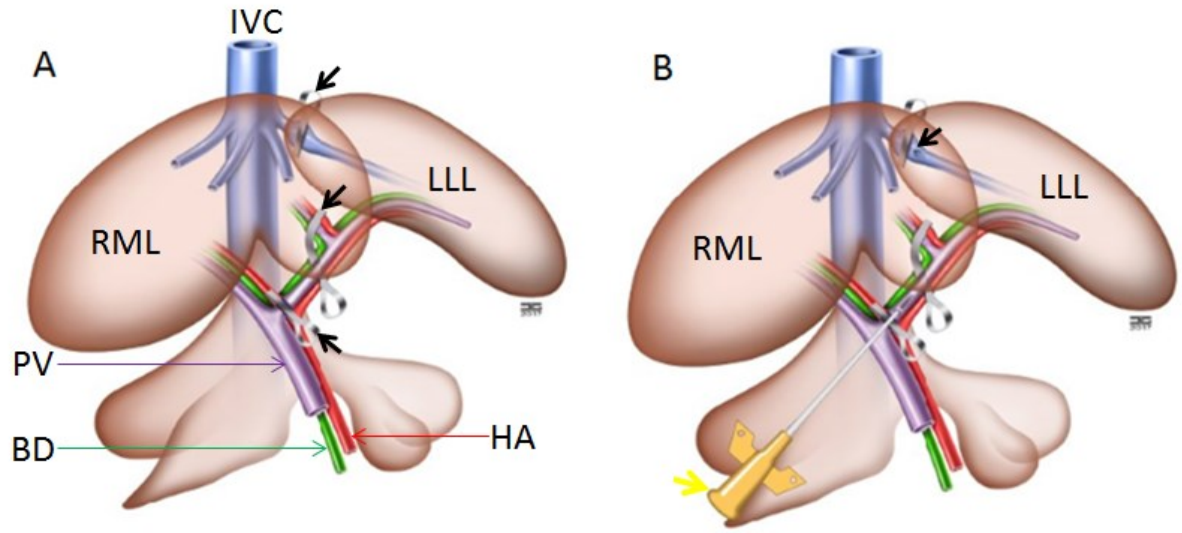

Figure 2. **A. Scheme of modified blockage of the vessels supplying and draining the LLL of rat liver.** The left PV is blocked with a pair of micro-clamps (lowest black arrow) at the base instead of using a suture line. The left HA, the left biliary tract along with the left lateral PV, the left lateral HA, and the left lateral BD are blocked with another pair of micro-clamps (median black arrow). The left lateral HV is blocked with a pair of micro-clamps (upper black arrow) as well. RML: Right median lobe. IVC: Inferior vena cava.

B. Scheme of modified generation of a selective bypass circulation through the LLL of rat liver. The left PV is cannulated with a 24G needle-free catheter as a fluid inlet (yellow arrow), and an incision opening (black arrow) is generated as a fluid outlet at the naturally exposed region of the front wall of the left lateral HV instead of using a catheter.

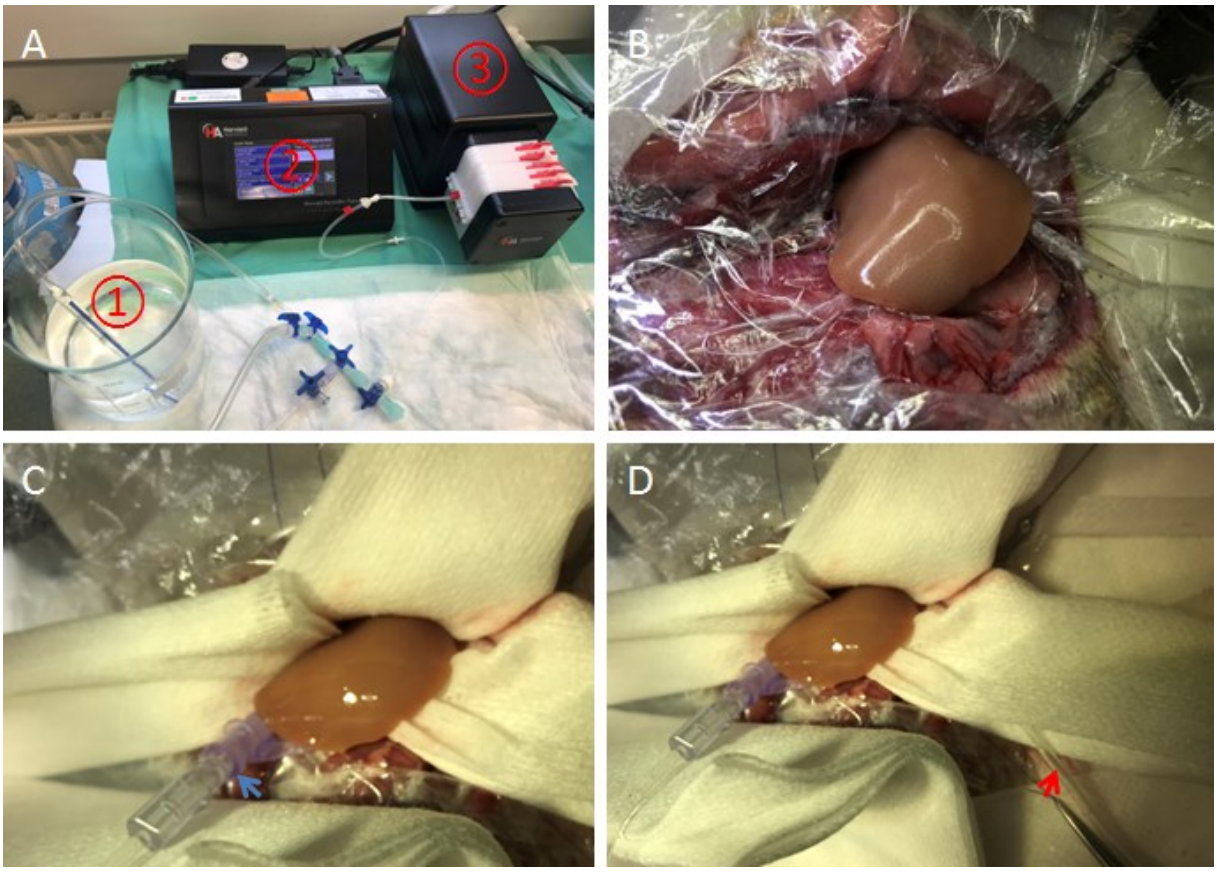

Figure 3. Intraoperative images showing perfusion system, isolation and drainage for in-vivo perfusion decellularization. Experimental set up with detergent solution (**A1**), a display (**A2**) and a peristaltic pump for perfusion (**A3**). Isolation of targeted LLL from other abdominal organs using PVDC film (**B**) and additional gauze (**C**) (an inlet catheter, blue arrow). Prevention of contamination by placing an additional aspiration tube (**D,** red arrow) between the gauze layer and by connecting to a suction device.

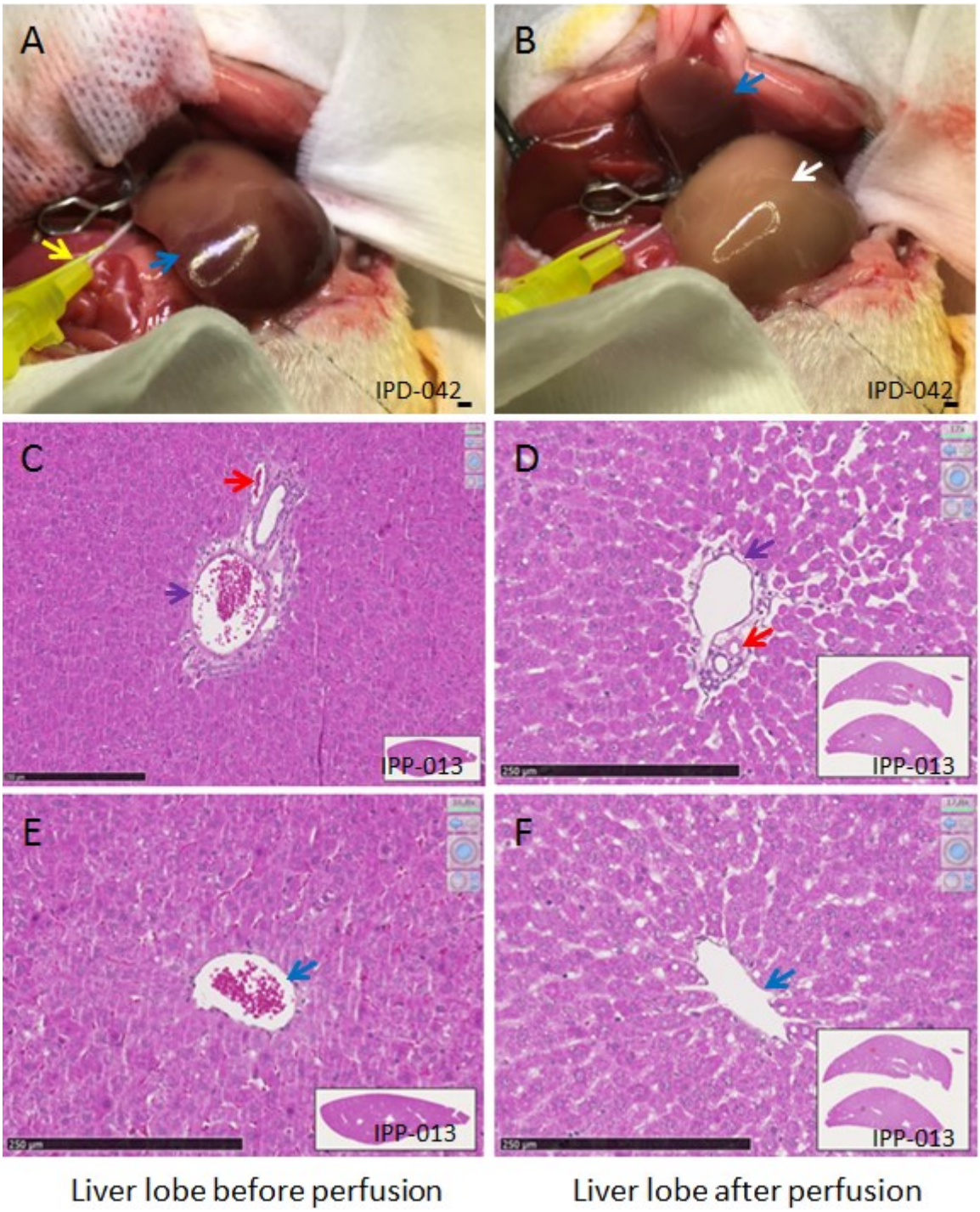

Figure 4. Confirmation of successful selective perfusion of LLL using the modified perfusion technique. A. Perfusion catheter (yellow arrow) in place after successfully blocking physiological perfusion to LLL as indicated by the dark red color (blue arrow). **B.** Color change of the LLL from dark red into faint yellow (white arrow) after perfusion with heparinized saline. Dark red showing the ischemia of the left median lobe (blue arrow). Scale bar=1 mm (**A-B**). **C.** Presence of blood cells in the PV (purple arrow), HA (red arrow), and

CV (**E**, blue arrow) of the normal liver lobe. **D**. Absence of blood cells in PV (purple arrow) and HA (red arrow) after heparin perfusion of left lateral liver lobe as well as in sinusoids and CV (**F,** blue arrow). Scale bar=250µm (**C-F**).

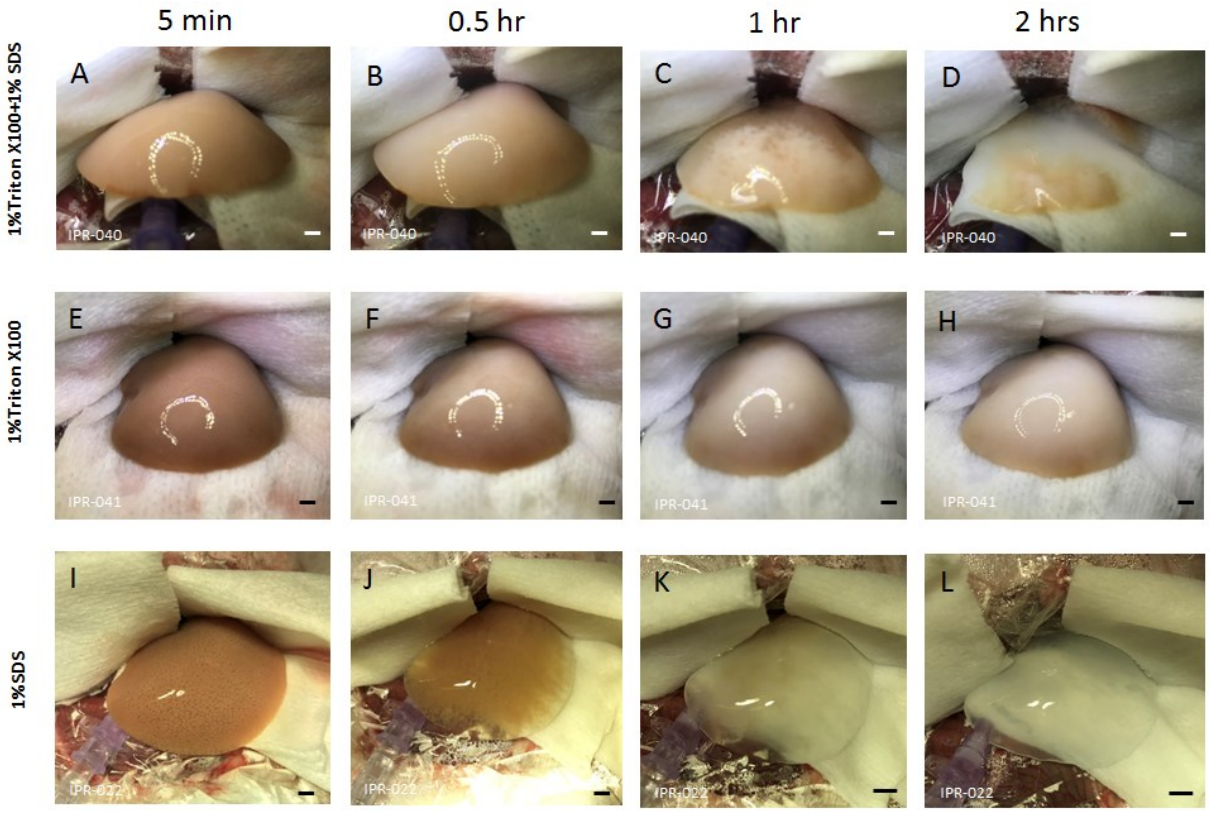

Figure 5. Intraoperative images showing in-vivo decellularization of the LLL. Time sequence from 5min to 2 hours using 1% Triton X100 followed by 1% SDS resulting in incomplete decellularization of the lobe (**A-D**). And 1% Triton X100 only resulting in colour change of the liver lobe (**E-H**). In contrast, 1% SDS only showing a gradual increasing transparency of the LLL (**I-L**). Scale bar=1 mm (**A-L**).

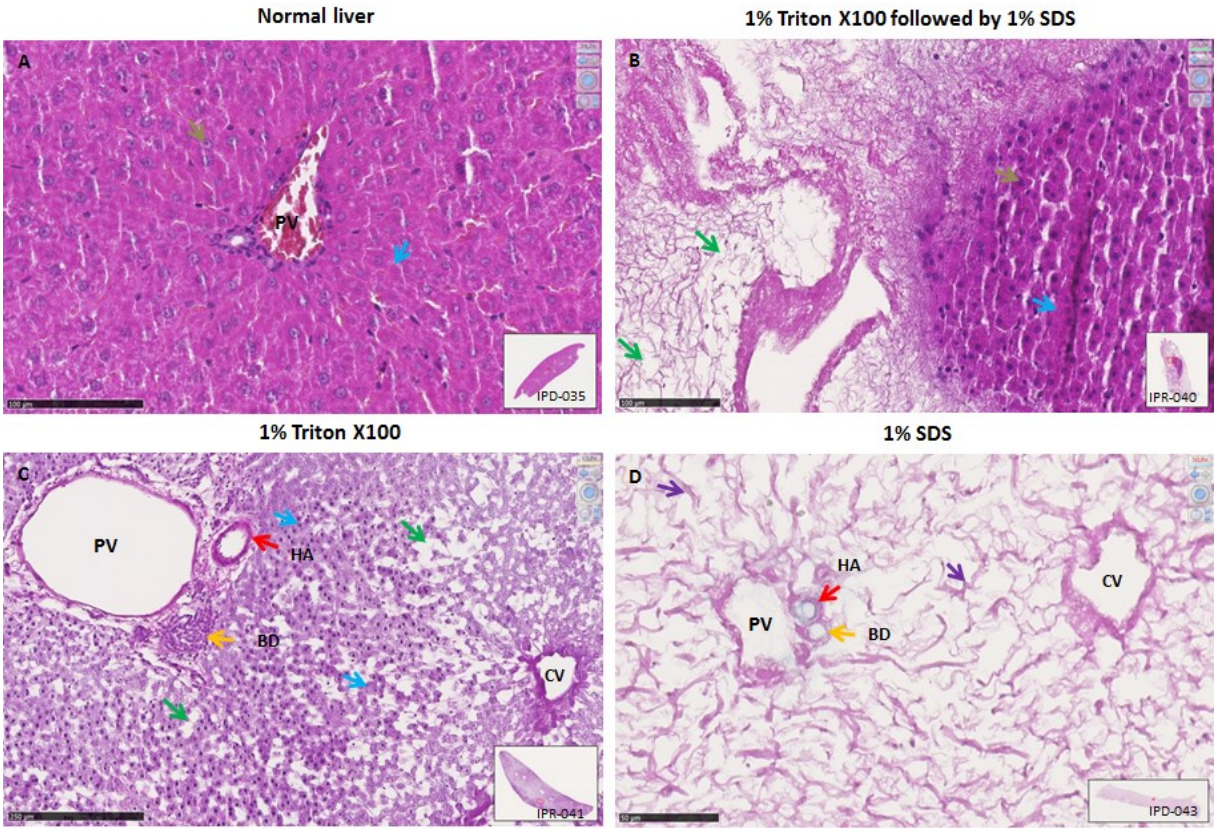

Figure 6. Histological assessment (HE) of scaffolds comparing three in-vivo decellularization protocols. A. Normal liver with blue-black staining nuclei (brown arrow) and purplish red staining cytoplasma (blue arrow). Scale bar 250um. **B**. Liver subjected to 1% Triton X100 followed by 1% SDS perfusion resulting in incomplete decellularization with cell-free areas (green arrows) but also areas with remnant hepatic parenchyma (brown arrows) and cytoplasma (blue arrow). Scale bar 100um. **C.** Liver subjected to only 1% Triton X100 perfusion resulting in incomplete decellularization with few cell-free spaces (green arrows) and only the changed colour of the other cells (blue arrows). HA (red arrow). BD (yellow arrow). Scale bar 250um. **D.** Liver subjected to only 1% SDS perfusion resulting in complete removal of hepatic cells while preserving collagen (pale pink) leaving the hepatic microarchitecture intact. Sinusoidal network (purple arrows). HA (red arrow).BD (yellow arrow). Scale bar 50um.

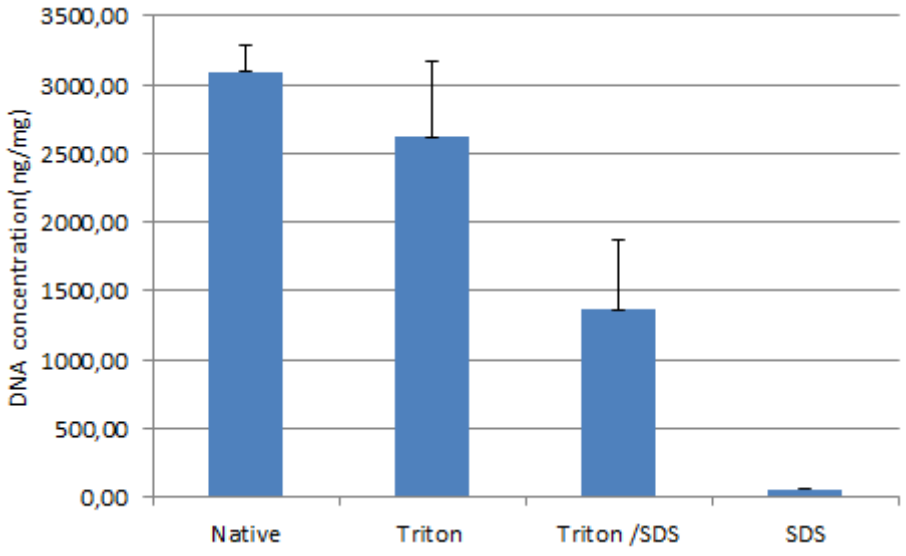

Figure 7. Molecular assessment of the decellularized scaffolds

DNA quantification of the decellularized liver scaffolds among the three groups of Triton X100 only, Triton X100 followed by SDS and SDS only, in comparison with that of native liver lobe.

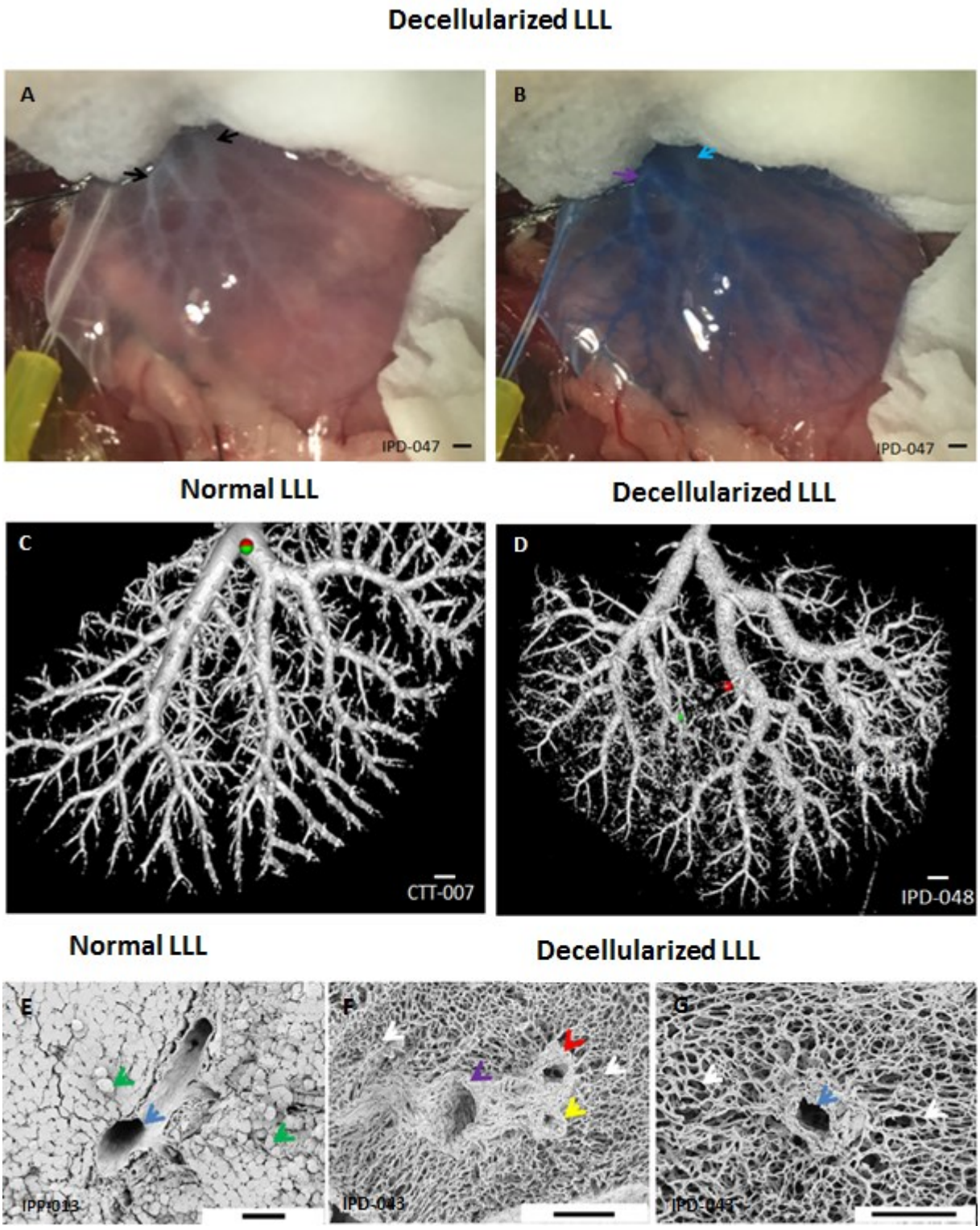

Figure 8. Characterization of structural architecture of the LLL scaffold. (**A**) Vascular trees appearing as white non-translucent structures (black arrows) in translucent scaffold after successful decellularization using 1%SDS for 2h. (**B**) Visualization of portal vascular tree (purple arrow) after injecting blue silicone contrast medium leaving the hepatic vascular tree uncontrasted (blue arrow). (**C**) Micro-CT scanning images showing intact portal vascular tree

of the decellularized left lateral scaffold comparable to (**D**) the portal tree of the native LLL. (**E**) SEM demonstrating the ultrastructure of native liver with CV (blue arrow) and cubical hepatocytes (green arrows). And (**F**) the acellular matrix of PV (purple arrow), HA (red arrow), BD (yellow arrow) and sinusoidal network (white arrows) presented in the decellularized scaffold. (**G**) Ultrastructure of CV (blue arrow) and hepatocyte-shaped free spaces surrounded with sinusoidal network structure (white arrows). Scale bar=1 mm (**A-D**), and 50 µm (**E-G**).

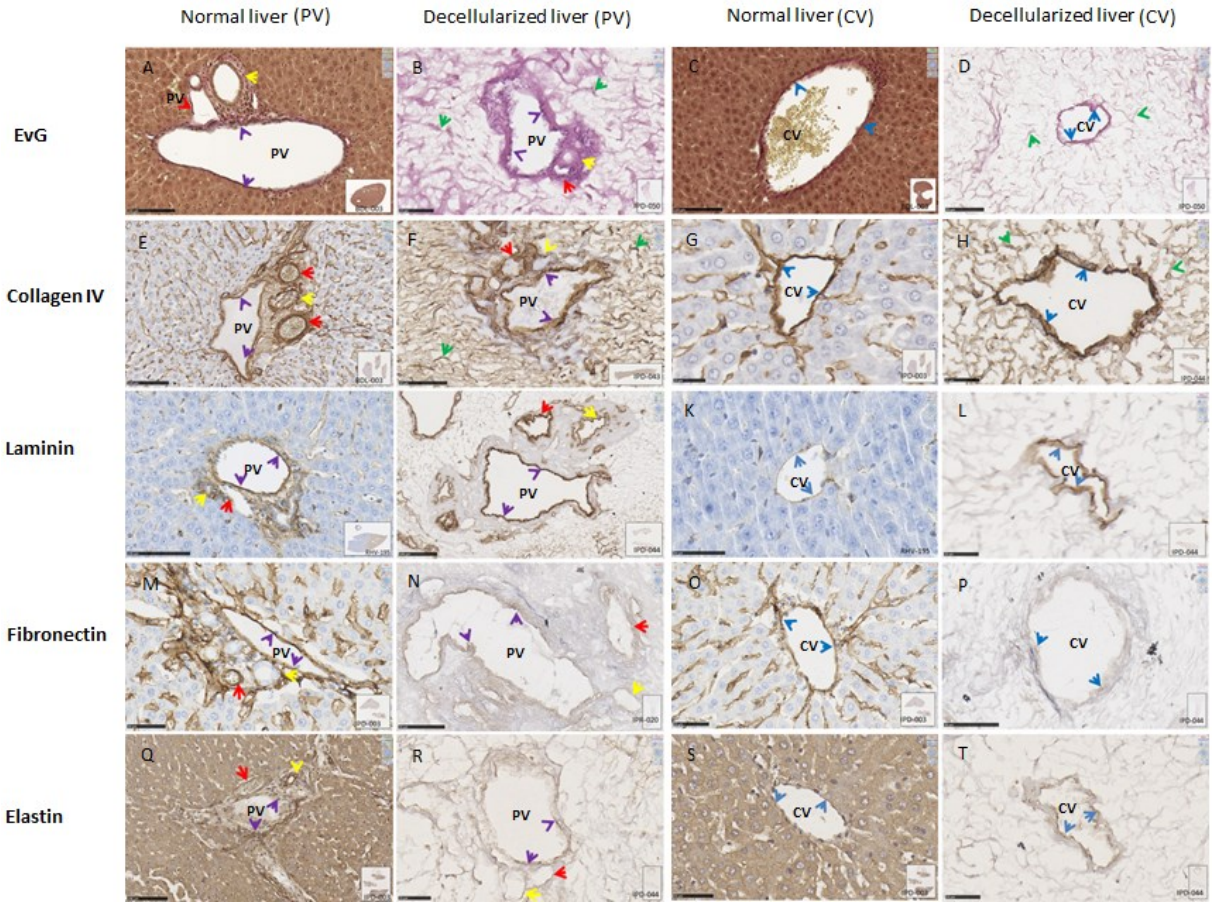

Figure 9. EvG staining and immunohistochemical assessment of the decellularized scaffold demonstrating the preservation of key extracellular matrix proteins in the portal field as well as the CV . In normal liver and decellularized liver scaffold and lobe, **EvG** staining showing red collagen (**A-D**) in the portal field including the PV (PV, purple arrows), the HA (red arrow), and the BD (yellow arrow), as well as in the CV (blue arrows)

and the sinusoid networks (green arrows). Immunohistological staining of structural matrix proteins in normal liver and scaffold demonstrating the preservation of collagen IV (**E-H)**, laminin (**I-L)**, fibronectin (**M-N)**, and elastin (**Q-T)** by the brown signal in the portal fields, and the CVs (blue arrows) as well as in the sinusoidal networks (green arrows). Scale bar=100 µm (**A, C, E, M** and **Q**), 50 µm (**D, F, K, M, N, O, P and S**) and 25 µm (**B, G, H, J, L, R and T**).

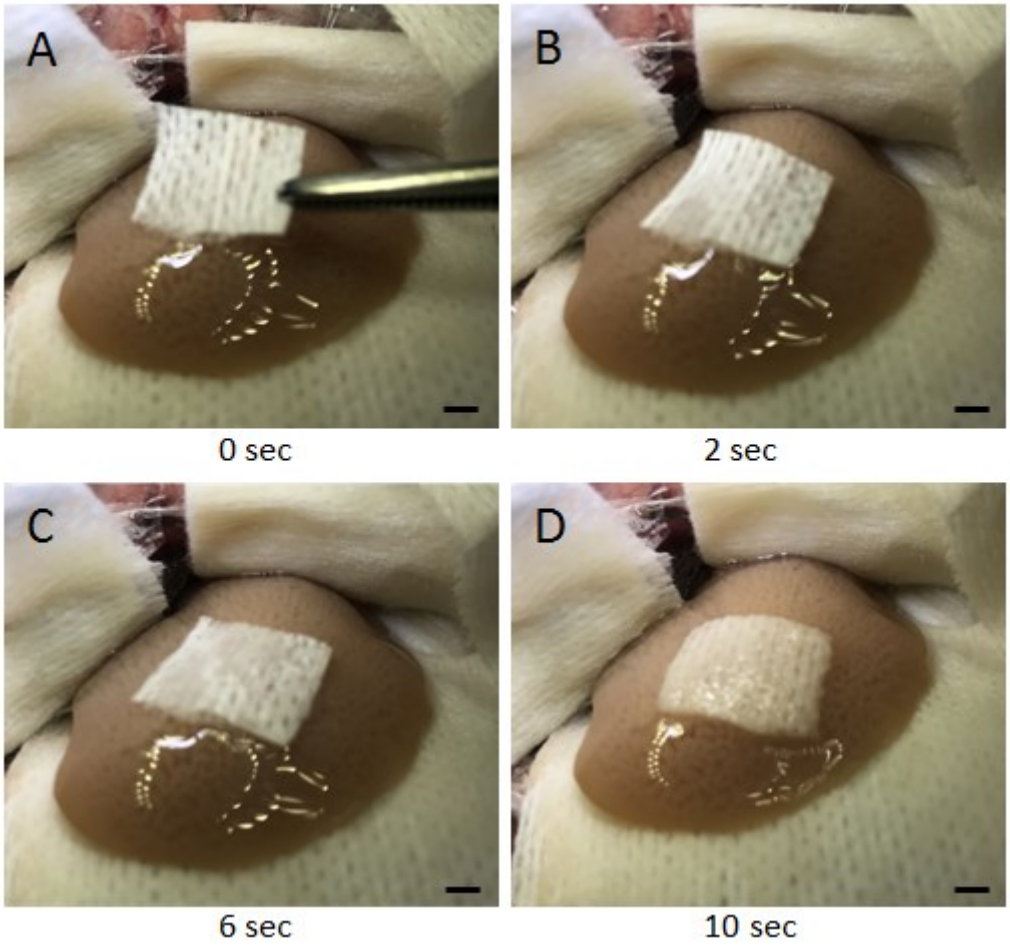

Figure 10. Intraoperative images showing waste perfusate emerging from the whole surface of the LLL during perfusion decellularizaton in-vivo.

A small square piece of dry gauze placed on the surface of the LLL turning from dry to wet within seconds (**A-D**) during in-vivo perfusion decellularization. Scale bar=1 mm.

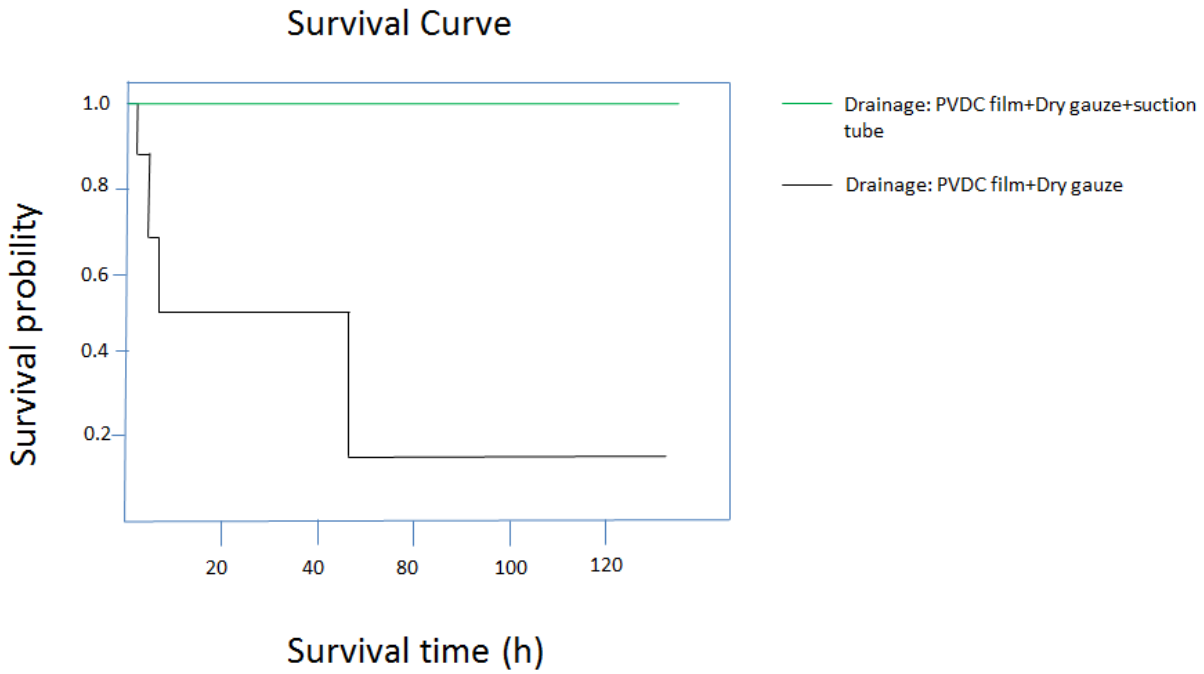

Figure 11. Survival rate of the rats between two different drainage methods

Kaplan-meier survival curve of the rats that subjected to the efficient drainage method of PVDC film+Dry gauze +suction tube and those that subjected to the less efficient drainage method (PVDC film+Dry gauze) during the procedure of in-vivo decellularization.

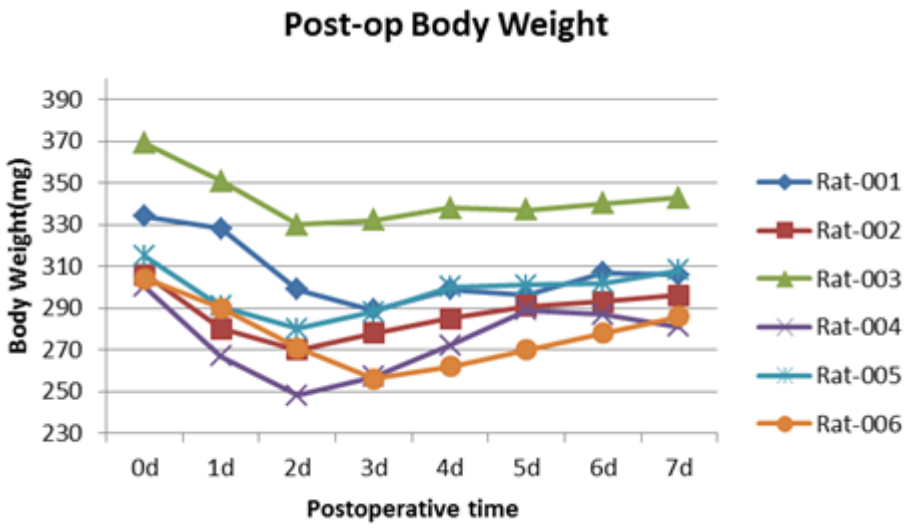

Figure 12. Postoperative body weight

A postoperative first-week observation of body weight of the rats subjected to the drainage method of PVDC film+Dry gauze +suction tube

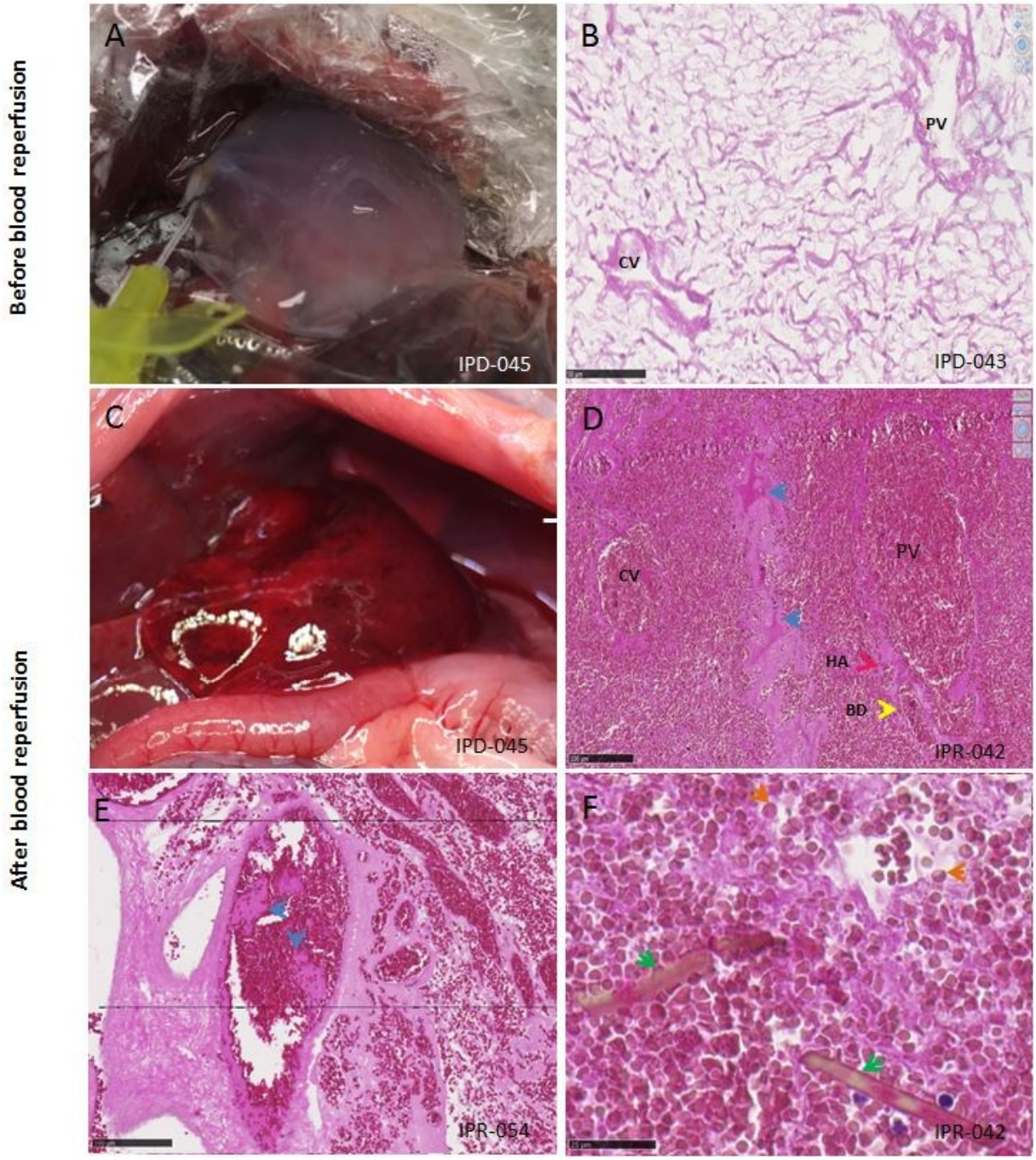

Figure 13. Physiological reperfusion of LLL scaffold in-vivo

(**A**) In-vivo image of translucent scaffold before and (**B**) blood filled scaffold immediately after reperfusion. Scale bar= 1 mm.

(**C**) HE-Staining of decellularized scaffold before and (**D**) blood filled scaffold 12h after reperfusion. Erythrocytes accumulating in distended large vessels (PV and CV) as well as in HA (red arrow), in the compressed sinusoidal network and in the BD (yellow arrow). Blood clots (**D-E,** blue arrows), altered swollen erythrocytes (**F,** brown arrows) as well as hemoglobin crystals (**F,** green arrows) in some areas of the sinusoidal network and vessels. Scale bar= 25 µm (**F**), 50 µm (**B**) and 100 µm (**D-E**).

Methods	Treatment 1 (Pretreatment)	Treatment 2 (Decellularization)	Treatment 3 (Drainage)	Animal number	Parameters
Modification of selective perfusion technique to make it suitable for in-vivo decellularization	LLL perfusion with 15ml 40U/ml heparin saline	/	Dry gauze	N=3	Macroscope, Histology
Comparison of three detergents for in-vivo perfusion decellularization	LLL perfusion with 15ml 40U/ml heparin saline	1%Triton X100 followed by 1%SDS	Plastic film+dry gauze	N=6	Macroscope, Histology, D N A quantification
		1%Triton X100 only	Plastic film+dry gauze	N=6	Macroscope, Histology, D N A quantification
		1% SDS only	Plastic film+dry gauze	N=6	Macroscope, Histology, D N A quantification,
Characterization of the scaffold fabricated by 1%SDS decellularization	LLL perfusion with 15ml 40U/ml heparin saline	1% SDS only	Plastic film+dry gauze	N=3	CT scan
				N=2	SEM
		/	/	N=1, as a normal control	CT scan
				N=1, as a normal control	SEM
Comparison of two drainage methods to eliminate waste fluid during in-vivo perfusion decellularization	LLL perfusion with 15ml 40U/ml heparin saline	1% SDS only	Plastic film+dry gauze	N=6	Survival analysis
		1% SDS only	Plastic film+dry gauze+aspiration tube	N=6	Survival analysis
Physiological reperfusion of the decellularized scaffold in-vivo	LLL perfusion with 15ml 40U/ml heparin saline	1% SDS only	Plastic film+dry gauze+aspiration tube	N=3	Macroscope, Histology

Table 1. Rats used for establishment of in-vivo partial liver lobe decellularization

Discussions

Generation of an in-vivo biological scaffold using in-vivo perfusion technique has become a promising strategy to study in-vivo liver engineering.

Our technique is the further development of the technique presented by Pan and offers a number of advantages:

First, preserving of the three main vessels and the bile duct allows physiological blood reperfusion as well as bile drainage of a liver lobe scaffold in-vivo. In previous other studies, only portal and hepatic vein but not bile duct and hepatic artery were re-anastomosed when attempting to transplant an ex-vivo engineered repopulated scaffold [Uygun 2010, Bao 2011, Katdota et al 2014, Bruinsma 2015, Ko et al 2015 and Hussein 2016]. In contrast, we preserved the left portal vein, left hepatic artery and left lateral central vein, as well as the left bile duct of the targeted decellularized liver lobe in-vivo. This is potentially critical for maintaining the viability of cells and the hepatic function after cells repopulation of a scaffold in-vivo.

Second, selecting the left lateral lobe instead of the right lobe enabled to maintain physiological perfusion of about 70% of the liver throughout the whole procedure. We did not block portal vein and vena cava, thereby preventing portal hypertension and intestinal congestion.

Third, reducing the harshness of the standard detergent protocol by perfusion with 1 % SDS only without the use of triton X resulted in a remarkable scaffold quality. We confirmed the results of other studies that SDS alone was of advantage in terms of decellularization time, DNA removal and ECM protein preservation [Uygun 2010 and Sullivan 2012]. Although SDS can damage ECM, previous studies showed that SDS can not only remove the immunogenic cellular components but also better retain the ECM constituents, compared to Triton X [Hussein 2013, Park 2013, Kadota 2014, and Hussein 2015].

Forth, ensuring efficient protection of the abdominal organs was achieved by minimizing detergent-induced corrosive injury. We used a PVDC-film to isolate the organs from the detergent and placed placing a suction tube in addition to dry gauze to efficiently drain the waste fluid.

Fifth, completing the whole procedure in less than 3h left approximately 2h for later reseeding the scaffold without exceeding the maximally tolerated operation time for about 5h. We flushed the liver lobe with heparin saline before in-vivo decellularization to prevent disseminated intravascular coagulation but also to dissolve small thrombi formed in the vessel, thereby accelerating the process of decellularization.

Altogether, we confirmed that the procedure of in-vivo selective liver lobe decellularization was not only well tolerated by the animals but also resulted in the complete removal of cellular components and a remarkably high scaffold quality.

Thus, we consider having achieved the next step on the road to in-vivo liver engineering, a technique very suitable to achieve a better understanding of scaffold repopulation.

However, there is still a major challenge to overcome: the prevention of coagulation in native liver scaffold upon reperfusion with blood. Therefore, we already considered the following options to reduce the thrombogenicity of the scaffold**:**

Manuscript III in preparation

1. Reseeding with endothelial cells

Repopulating the scaffold with endothelial cells is supposed to be capable of preventing coagulation. Reseeding the scaffold with endothelial cells can naturally cover the surface of collagen inside the scaffold. Preventing collagen from being exposed to blood platelets and coagulation factors is preventing the initiation of the coagulation cascade.

However, according to our experience the total operation time should not exceed 5 hours. Subsequently, the time for reseeding endothelial cells in-vivo including the single or repeated application and eventual time for adherence should be limited to maximally additional 2 hours. Compared to ex-vivo re-endothelialization which needs several days [Uygun 2010, Ko 2015, Hussein 2016 and Devalliere 2018], this time frame is rather short. Furthermore, coverage of the vasculature through reseeding endothelial cells may be incomplete and uneven, resulting in areas potentially not covered with endothelial cells and remaining thrombogenic. These two limitations may result in an incomplete prevention of coagulation.

2. Systemic heparinization

Full heparinization is very effective in preventing coagulation. Heparin binds with high affinity to the protein antithrombin III, thrombin and coagulation factor Xa. Therefore, it is an

ideal bio-active agent for anticoagulation [Werner 2007]. However, to our knowledge, there are no reports regarding systemic heparinization for anticoagulation after blood reperfusion of a liver scaffold or engineered liver grafts in-vivo. To prevent coagulation efficiently, full heparinization would be needed. However, this may cause bleeding from the in- and outlet as well as from the base of the liver lobes previously clamped.

3. Local heparinization

Recently, local heparinization has been used for anticoagulation through directly flushing the decellularized scaffold with heparin. Heparin immobilized in a decellularized bioscaffold acts as an antithrombotic coating reagent and binds vascular endothelial growth factor (VEGF) to induce angiogenesis in the scaffolds [Kidane 2004, You 2011, Bae 2012 and Wei 2013].

3.1 Layer by layer heparin coating technique

For Layer by layer heparinization technique, the luminal surface (negatively charged) of the biological scaffold is covered with positively charged polyelectrolyte followed by a negatively charged heparin solution. This sequence is repeated several times forming a multilayer film adhering together by electrostatic force. This interesting technique was already used successfully in some studies to prevent coagulation when transplanting a repopulated liver scaffold [Bao 2011, Bao et al 2015, and Bruinsma 2015].

3.2 Own experiences:

Therefore, we did first pilot experiments for preventing coagulation using the layer by layer heparin coating technique modified from Bao [Bao 2011]. After in-vivo left lateral lobe decellularization, we washed the liver lobe for 10 min with 50 ml 0.9% sodium chloride to remove residual 1% SDS. To prevent coagulation, prior to blood reperfusion of the scaffold, we perfused the liver scaffold with 5ml polyelectrolyte polydiallyldimethylammonium chloride (PDADMAC, 1g/L, Mw=100-200 kDa,), and 5ml 0.9% sodium chloride for rinsing, followed by 5ml heparin saline (2g/L) and repeated the three steps for three times.

Afterwards, we reperfused the scaffold in-vivo with autologous blood by releasing the clamps to reopen the vessels. We checked the base of the decellularized liver lobe for bleeding since the clamps obviously damaged the parenchymal tissue before closing the abdomen. Minimal small bleeding was observed. This small bleeding did stop upon light compression due to the physiological initiation of coagulation and allowed long term survival of the animals. This was shown after in-vivo selective liver lobe perfusion with saline [Wang 2018] and after in-

vivo selective liver lobe decellularization as described in manuscript II. However after local heparinization all rats (n=6/6) died within 48 hours, as seen in **Figure 1**, due to bleeding as observed upon autopsy. The bleeding site was at the base of the scaffold damaged by the micro-clamps used during in-vivo decellularization. Apparently, the minimal bleeding was not fully stopped by compression in the absence of coagulation but must have restarted after closing the abdomen, finally causing the death of the animal.

Histological samples taken whenever the animals died allowed us to monitor the interaction of blood perfusion and the scaffold itself over time for up to 48hours. We observed **three major findings:** invasion of erythrocytes and formation of hemoglobin crystals as well as neutrophil infiltration in both the vessels and sinusoidal network.

In all samples **(Fig. 2A-D)** major vessels were full of erythrocytes. However, the amount of blood in the sinusoidal network did vary within the scaffold suggesting inhomogeneous reperfusion, with a tendency to fewer erythrocytes at the early time point (1h). No blood clots were seen suggesting that the layer-by-layer heparinization was successfully preventing the initiation of coagulation.

In contrast, we observed damaged erythrocytes appearing translucent and colorless and often with distorted rather rectangular shape. Interestingly, in the majority of samples **(Fig. 2C-F)**, we detected long almost translucent crystalloid structures in the blood vessels, but also in the sinusoidal network. Some of them appeared yellowish and others more reddish, possibly representing crystalloid hemoglobin aggregates. Two arguments are in favor of this interpretation: First, Bielawski reported already in 1989, that SDS, even in concentrations as low as 0.003 to 0.001% causes hemolysis of a certain number of erythrocytes [Bielawski 1990]. Furthermore, he showed that resistance of erythrocytes decreases with temperature. Rinsing the scaffold for 5 min with 50ml of 0.9% sodium chloride solution might not be sufficient to dissociate all SDS bound to the collagen in the scaffold. Second, formation of hemoglobin crystals was reported after toxic lung [Ghio et al. 2000, Paakko et al. 1996 and Zachary et al. 2001] and kidney [Madsen et al. 1982] injury. Hemoglobin crystals were also observed in the brain of rats, as seen in **Fig. 2G-H** taken from Kleinig [Kleinig, 2009], after inducing intracranial hemorrhage. In our case crystal formation might be due to a similar toxic effect of the residual SDS bound to scaffold proteins and not covered by the subsequent layer by layer heparinization.

Previous experiments obtained after ex-vivo layer by layer heparinization in liver scaffold and prior to in-vivo did not reveal this phenomenon [Bao 2011 and Bruinsma 2015]. However, scaffolds were rinsed with PBS [Bruinsma 2015 and Devalliere 2018] or antibiotic-containing physiological saline [Bao 2011] more extensively for one or several hours prior to heparinization, not feasible in our in-vivo situation. Therefore we consider improving the SDS-wash-out step by adding proteins to the rinsing solution and by prolonging the rinsing step of the scaffold to better remove residual SDS [Devalliere 2018].

Furthermore, over time, we observed an increasing amount of white blood cells infiltrating the scaffolds **(Fig. 2E-F)**. The relative frequency of neutrophils increased from the expected ratio of 1:1000 white blood cells to red blood cells observed at 3h to a dense predominantly neutrophilic infiltrate located in between the hemoglobin crystals and the compressed scaffold structure. This could be as least partially due to the pro-inflammatory role of hemoglobin crystals suggested by Kleinig [Kleinig 2009]. However, this might not be the only reason for the inflammatory reaction within the scaffold.

Figure 1

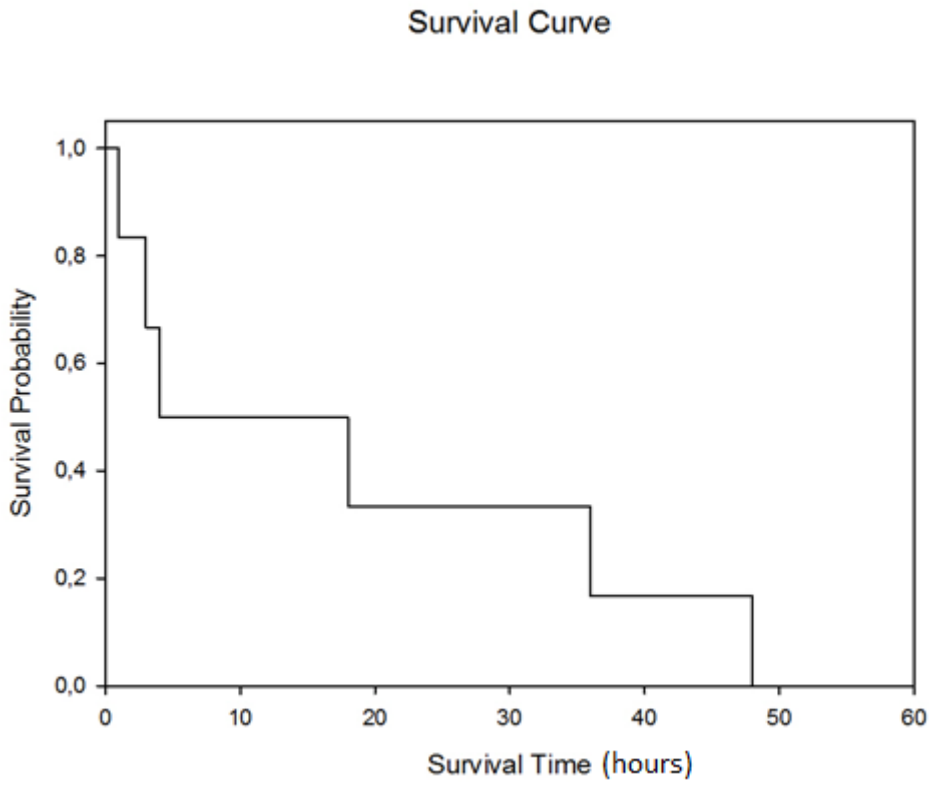

Figure 1. Kaplan-Meier survival curve of the rats that underwent layer by layer local heparinization of decellularized scaffold followed by in-vivo blood reperfusion.

Figure 2

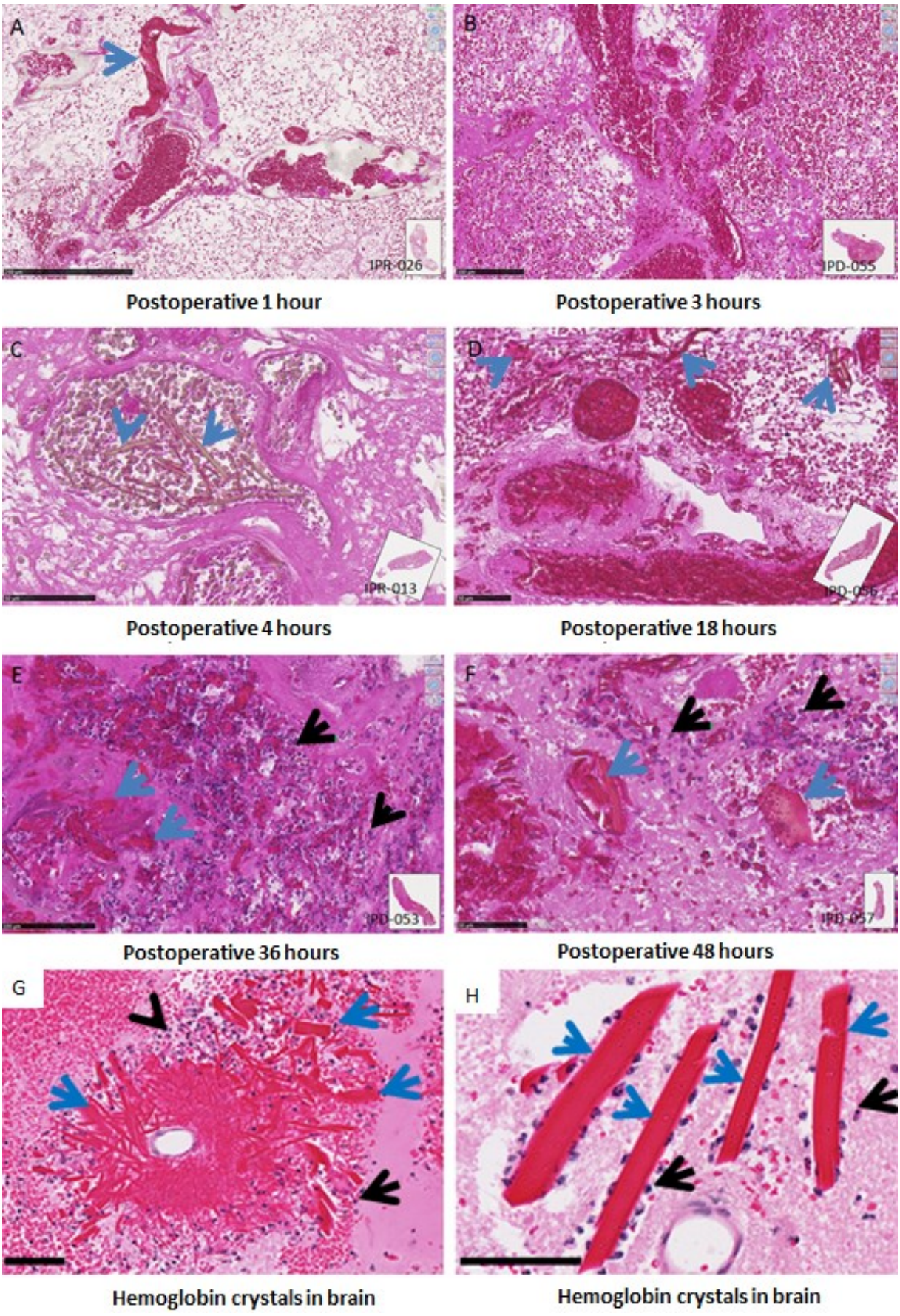
A
IPR-026
Postoperative 1 hour
B
IPD-055
Postoperative 3 hours
C
IPR-013
Postoperative 4 hours
D
IPD-056
Postoperative 18 hours
E
IPD-053
Postoperative 36 hours
F
IPD-057
Postoperative 48 hours
G
Hemoglobin crystals in brain
H
Hemoglobin crystals in brain

Figure 2. Histological assessment (H&E staining) of scaffolds after local layer by layer heparinization followed by blood reperfusion. (**A-D**) Large amounts of **erythrocytes** were visible in the large vessels of all reperfused heparin-treated liver scaffolds and to a variable extent also in the sinusoidal network. (**A** and **C-F**) **Hemoglobin crystals** (blue arrows) were observed in almost all scaffolds (1h, 4h, 18h, 36h and 48h), albeit in different extent, very little early after reperfusion and more in the later phase. (**E-F**) Large amounts of **white cells** infiltrating the parenchymal space (black arrows) along with hemoglobin crystals (blue arrows) were visible in the blood reperfused heparin-treated scaffold at postoperative 36 h and 48 h. Hemoglobin crystals looked similar to the ones observed similar to (**G-H**) hemoglobin crystals (blue arrows) and white cells (black arrows), the ones observed in the brain of rats 24 h after intracerebral hemorrhage as described by Kleinig [Kleinig 2009]**.** Scale bar 50 μm (**C, D** and **F**). Scale bar 100 μm (**B, E** and **G-H**). Scale bar 100 μm (**A**).

Balance between inhibition of coagulation and risk of bleeding

Taking our observations together, we observed clotting in the scaffold when reperfusing the scaffold without preventing coagulation. However, we encountered lethal bleeding when using layer-by-layer heparinization. It seems very hard to achieve the delicate balance between ensuring efficient anticoagulation within the scaffold and inducing severe bleeding from the damaged, previously clamped base of the liver lobe scaffold. Therefore we evaluated the use of local hemostatics.

We first covered the damaged region of the heparin-treated scaffold immediately after releasing the clamps with sealant matrix, (Tachosil, Baxter, German) (**Fig.3A**). However, when waiting for a prolonged period of time (10-20min), we could still observe minimal, but constant bleeding from the very small uncovered surface of the scaffold base. Complete coverage, especially in between the left lateral portal vein and hepatic vein was difficult to achieve due to the large size and stiff property of the matrix in respect to the tiny uncovered area of the base ($<1mm^2$).

To achieve better coverage, we then tried to apply a liquid fibro sealant (**Fig. 3B**) (Tisseel, Baxter, German), but with similar result of minimal but constant bleeding. As a next step we first applied the matrix and the liquid sealant in addition (**Fig.3C**) which also did not prevent bleeding. As a last step we tried to prevent bleeding by completely covering the scaffold Tachosil (**Fig.3D**), however without improving the result.

Figure 3

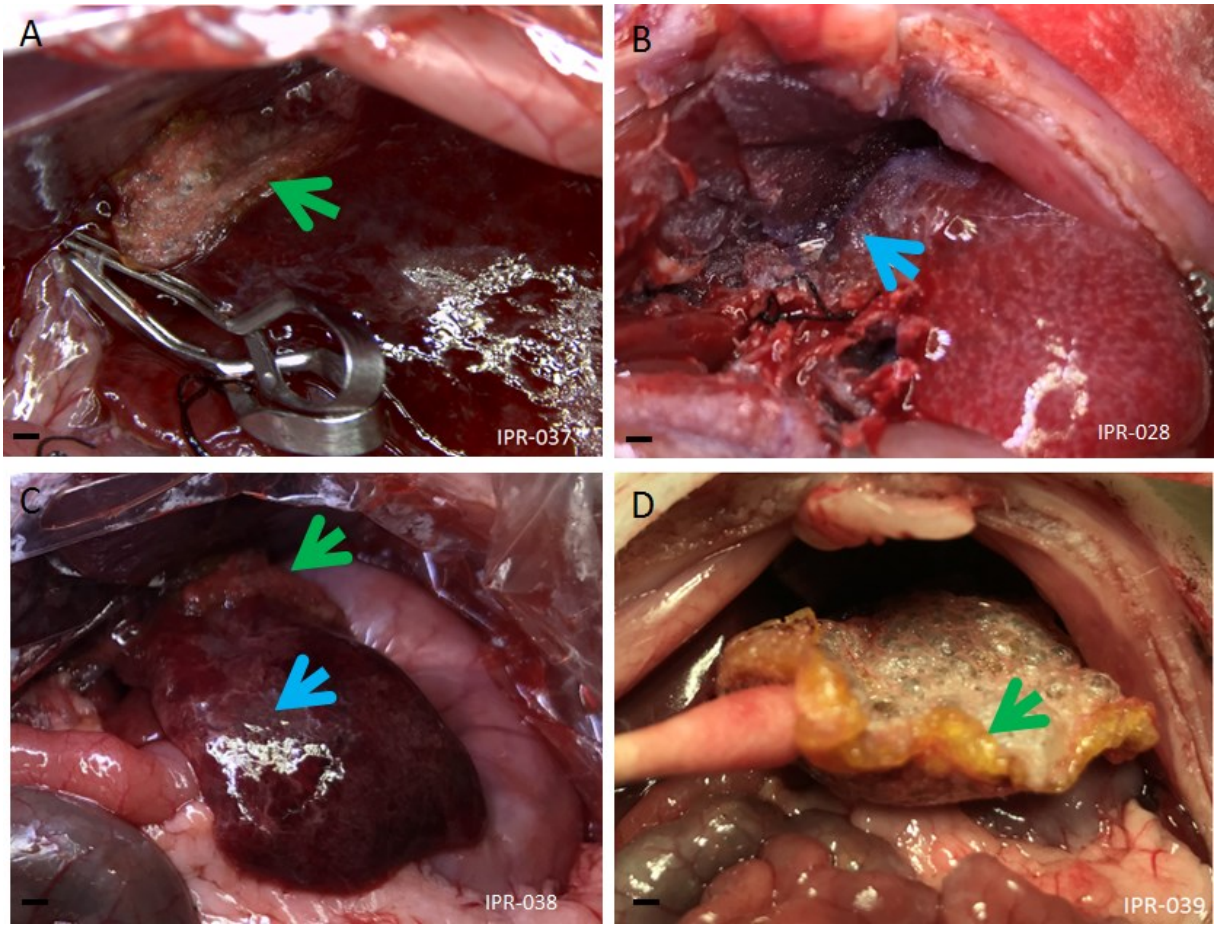

Figure 3. Intraoperative images showing in-vivo coagulation using hemostatics after local heparinization followed by blood reperfusion of the left lateral lobe scaffold. **A.** Applying solid sealant matrix (green arrow), onto the damaged region of the heparin-treated scaffold immediately after releasing the clamp from the hepatic artery. **B.** Putting a liquid fibro sealant (blue arrow) instead of solid sealant matrix to the bleeding scaffold. **C.** Applying both solid sealant matrix (green arrow) and liquid fibro sealant (blue arrow) onto the scaffold. **D.** Covering the whole surface of the liver scaffold with solid sealant matrix (green arrow). Scale bar=1 mm (**A-D**).

Other authors used the layer by layer heparin coating technique after ex-vivo liver decellularization. They reported efficient prevention of coagulation, but no bleeding problems within the observation time of up to 72h [Bao 2011, Bao et al 2015 and Bruinsma 2015]. However, they only applied the heparin into a scaffold without injury. In contrast, in-vivo selective liver lobe decellularization leads to a small but unavoidable relevant parenchymal damage at the base of the decellularized liver lobe by the clamps used.

Therefore we must conclude that local heparinization was not only effectively preventing coagulation within the scaffold, but resulted in lethal bleeding at the damaged base of the scaffold. Furthermore, using sealant matrix or liquid fibro sealant or both did not efficiently

stop bleeding from the physiologically reperfused scaffold and also did not prolong the life span of the animals. Thus these findings call for evaluating other methods potentially preventing coagulation in the scaffold without increasing the risk of bleeding at the base of the scaffold.

3.3 Heparin-gelatin mixture coating technique

In a previous study, heparin-gelatin mixture coating of decellularized pig liver scaffold via portal vein and hepatic artery ex-vivo did decrease thrombogenicity confirmed by contrast angiography after the scaffold was subjected to ex-vivo blood perfusion. It also increased migration and attachment of endothelial cells to the vessel wall after re-endothelialization ex-vivo. However, it took as long as 2 hours for infusion of heparin-gelatin mixture and incubation [Hussein 2016].

Therefore we are going to try this as next step with or without adding local hemostastics. If this would solve the problem, this would call for applying the cells together with the local anticoagulative treatment to achieve repopulation.

Conclusion

In brief, we established a surgical perfusion model of selective left lateral liver lobe in-vivo in rat. We also presented a survival model of in-vivo left lateral liver lobe decellularization in rat resulting in the complete removal of cellular components, yielding a high quality scaffold suitable for the subsequent physiological reperfusion.

Preliminary experiments were directed towards achieving the delicate balance between preventing coagulation within the scaffold without increasing the risk for bleeding at the base of the scaffold. Therefore, as a next step we will evaluate other local anticoagulation strategies such as the heparin-gelatin mixture coating technique.

Once these two challenges are resolved, we will explore in-vivo recellularization of the liver scaffold with hepatocytes and non-parenchymal cells.

References

Bae, I.H., et al., *Thromboresistant and endothelialization effects of dopamine-mediated heparin coating on a stent material surface.* J Mater Sci Mater Med, 2012. **23**(5): p. 1259-69.

Bao, J., et al., *Construction of a portal implantable functional tissue-engineered liver using perfusion-decellularized matrix and hepatocytes in rats.* Cell Transplant, 2011. **20**(5): p. 753-66.

Bao, J., et al., *Hemocompatibility improvement of perfusion-decellularized clinical-scale liver scaffold through heparin immobilization.* Sci Rep, 2015. **5**: p. 10756

Bielawski, J., *Two types of haemolytic activity of detergents.* Biochim Biophys Acta, 1990. **1035**(2): p. 214-7.

Bruinsma, B.G., et al., *Layer-by-layer heparinization of decellularized liver matrices to reduce thrombogenicity of tissue engineered grafts.* J Clin Transl Res, 2015. **1**(1).

Devalliere, J., et al., *Improving functional re-endothelialization of acellular liver scaffold using REDV cell-binding domain.* Acta Biomater, 2018. **78**: p. 151-164.

Ghio, A.J., et al., *Iron disequilibrium in the rat lung after instilled blood.* Chest, 2000. **118**(3): p. 814-23.

Hussein, K.H., et al., *Heparin-gelatin mixture improves vascular reconstruction efficiency and hepatic function in bioengineered livers.* Acta Biomater, 2016. **38**: p. 82-93.

Hussein, K.H., et al., *Sterilization using electrolyzed water highly retains the biological properties in tissue-engineered porcine liver scaffold.* Int J Artif Organs, 2013. **36**(11): p. 781-92.

Hussein, K.H., et al., *Construction of a biocompatible decellularized porcine hepatic lobe for liver bioengineering.* Int J Artif Organs, 2015. **38**(2): p. 96-104.

Jiang, W.C., et al., *Cryo-chemical decellularization of the whole liver for mesenchymal stem cells-based functional hepatic tissue engineering.* Biomaterials, 2014. **35**(11): p. 3607-17.

Kadota, Y., et al., *Mesenchymal stem cells support hepatocyte function in engineered liver grafts.* Organogenesis, 2014. **10**(2): p. 268-77.

Kidane, A.G., et al., *Anticoagulant and antiplatelet agents: their clinical and device application(s) together with usages to engineer surfaces.* Biomacromolecules, 2004. **5**(3): p. 798-813.

Kleinig, T.J., et al., *Hemoglobin crystals: A pro-inflammatory potential confounder of rat experimental intracerebral hemorrhage.* Brain Research, 2009. **1287**: p. 164-172.

Kojima, H., et al., *Establishment of practical recellularized liver graft for blood perfusion using primary rat hepatocytes and liver sinusoidal endothelial cells.* Am J Transplant, 2018. **18**(6): p. 1351-1359.

Ko, I.K., et al., *Bioengineered transplantable porcine livers with re-endothelialized vasculature.* Biomaterials, 2015. **40**: p. 72-9.

Madrahimov, N., et al., *Marginal hepatectomy in the rat: from anatomy to surgery.* Ann Surg, 2006. **244**(1): p. 89-98.

Madsen, K.M., C.W. Applegate, and C.C. Tisher, *Phagocytosis of erythrocytes by the proximal tubule of the rat kidney.* Cell Tissue Res, 1982. **226**(2): p. 363-74.

Mussbach, F., et al., *Bioengineered Livers: A New Tool for Drug Testing and a Promising Solution to Meet the Growing Demand for Donor Organs.* Eur Surg Res, 2016. **57**(3-4): p. 224-239.

Mussbach, F., et al., *[Liver engineering as a new source of donor organs : A systematic review]*. Chirurg, 2016. **87**(6): p. 504-13.

Paakko, P., et al., *Biochemical and morphological characterization of carbon tetrachloride-induced lung fibrosis in rats.* Arch Toxicol, 1996. **70**(9): p. 540-52.

Pan, J., et al., *In-vivo organ engineering: Perfusion of hepatocytes in a single liver lobe scaffold of living rats.* Int J Biochem Cell Biol, 2016. **80**: p. 124-131.

Park, K.M., et al., *Preparation of immunogen-reduced and biocompatible extracellular matrices from porcine liver.* J Biosci Bioeng, 2013. **115**(2): p. 207-15.

Sullivan, D.C., et al., *Decellularization methods of porcine kidneys for whole organ engineering using a high-throughput system.* Biomaterials, 2012. **33**(31): p. 7756-64.

Uygun, B.E., et al., *Organ reengineering through development of a transplantable recellularized liver graft using decellularized liver matrix.* Nat Med, 2010. **16**(7): p. 814-20.

Wang, A., et al., *A Novel Surgical Technique As a Foundation for In Vivo Partial Liver Engineering in Rat.* JoVE, 2018(140): p. e57991.

Wei, H., et al., *Anticoagulant surface coating using composite polysaccharides with embedded heparin-releasing mesoporous silica.* ACS Appl Mater Interfaces, 2013. **5**(23): p. 12571-8.

Werner CMM, Sperling C. Current strategies towards hemocompatible coatings. J Mater Chem. 2007; 17:3376–3384.

Xie, C., et al., *Monitoring of systemic and hepatic hemodynamic parameters in mice.* J Vis Exp, 2014(92): p. e51955

You, I., et al., *Enhancement of blood compatibility of poly(urethane) substrates by mussel-inspired adhesive heparin coating.* Bioconjug Chem, 2011. **22**(7): p. 1264-9.

Zachary, J.F., et al., *Temporal and spatial evaluation of lesion reparative responses following superthreshold exposure of rat lung to pulsed ultrasound.* Ultrasound Med Biol, 2001. **27**(6): p. 829-39.

Acknowledgment

I would like to sincerely thank **Prof. Dr. Utz Settmacher**, Director of "Department of General, Visceral and Vascular Surgery, Friedrich-Schiller-University Jena Hospital" for giving me the chance to conduct research work and sparing no effort to support my work for years.

I would like to express my warmest thanks to my supervisor **Prof. Dr. Uta Dahmen**, the leader of "Experimental Transplantation Surgery, Department of General, Visceral and Vascular Surgery, Friedrich-Schiller-University Jena Hospital". I am grateful to her for offering me the opportunity to join into a great research team. She spent a lot of effort on designing and supervising my research project as well as provided constructive comments and criticisms throughout my study. In addition, she also gave me a lot of help for living in a foreign country. Her comments and suggestions on research or even on daily life will keep guiding me to the way of career.

I owe my gratitude to **Dr. Olaf Dirsch** for his generous help and guidance regarding histological evaluation of my study.

I want to give my gratitude and sincere compliments to **Weiwei Wei** as an excellent colleague and a nice friend, who introduced me into experimental microsurgery and giving valuable suggestions regarding surgical work.

I am thankful for **Isabel Jank**, who had already helped me before my arrival in Germany and her constant and kind helps in research work for language advices and in daily life for helping me solve problems all the time.

I would like to thank **Jens Geiling** from the Institute of Anatomy I, Jena University Hospital for providing me with excellent schematic drawings of rat liver anatomy.

I also want to thank **Dr. Felix Gremse** from Aachen for helping me with the scanning of explanted liver specimens and micro-CT data reconstructions.

Many thanks to **Dr. Sandor Nietzsche** for his continuous and great help in imaging ultrastructure of liver scaffold using SEM technique.

Sincerely thanks my kindly colleagues **Dr. Claudia Schindler** and **Olha Kuriata** for the great animal care, **Kathrin Schulz** and **Janine Arlt** for large amount of histological staining.

Sincerely thanks my colleagues **Dr.Philipp Felgendreff, Chuanfeng Hua, Fengming Xu,** and **Ana Lucia Paz** for an efficient teamwork. It is my pleasure to work with a great research team.

Last but not least, I would like to thank my family. I will never be successful without your support and encouragement.

Ehrenwörtliche Erklärung

Hiermit erkläre ich, dass mir die Promotionsordnung der Medizinischen Fakultät der Friedrich-Schiller-Universität bekannt ist,

ich die Dissertation selbst angefertigt habe und alle von mir benutzten Hilfsmittel, persönlichen Mitteilungen und Quellen in meiner Arbeit angegeben sind,

mich folgende Personen bei der Auswahl und Auswertung des Materials sowie bei der Herstellung des Manuskripts unterstützt haben: Isabel Jank, Weiwei Wei, Claudia Schindler und Uta Dahmen,

die Hilfe eines Promotionsberaters nicht in Anspruch genommen wurde und dass Dritte weder unmittelbar noch mittelbar geldwerte Leistungen von mir für Arbeiten erhalten haben, die im Zusammenhang mit dem Inhalt der vorgelegten Dissertation stehen,

dass ich die Dissertation noch nicht als Prüfungsarbeit für eine staatliche oder andere wissenschaftliche Prüfung eingereicht habe und

dass ich die gleiche, eine in wesentlichen Teilen ähnliche oder eine andere Abhandlung nicht bei einer anderen Hochschule als Dissertation eingereicht habe.

Ort, Datum Unterschrift des Verfassers

Curriculum Vitae

Experimental experience:

In-vivo partial liver perfusion in rat

In-vivo partial liver decellularization in rat

In-vivo physiologically reperfusion of partial liver scaffold in rat

Liver resection in rat: 30%, 70%, and 90%

Isolation of rat liver cells

Liver resection using the ALPPS (Associating Liver Partition and Portal vein Ligation for Staged Hepatectomy) method in rat

Liver vascular visualization (Microfil+micro CT imaging or Gadolinium+MRI imaging)

Software "HistoCAD VirtualLiver" for liver proliferation analysis

Software "IMALYTICS preclinical 2.0" for visual liver analysis

Software "Adobe premiere Pro CS6" for editing film

Western Blotting for proteins analysis

Enzyme-linked Immunosorbent Assay (ELISA) for cytokines analysis

Scientific Achievement:

Publications:

1. **An Wang1**, Olha Kuriata, Fengming Xu, Sandor Nietzsche, Felix Gremse, Olaf Dirsch, Utz Settmacher, Uta Dahmen.
   A survival model of in-vivo partial liver lobe decellularization towards in-vivo liver engineering. Tissue Engineering Part C. IF=2,63. Accepted. 27th, Sept 2019.

2. **An Wang,** Isabel Jank,Weiwei Wei, Claudia Schindler, Uta Dahmen.

A novel surgical technique as a foundation for in vivo partial liver engineering in rat. Journal of Visualized experiments. 2018 Oct. (IF=1.3)

3. Shen X , Jin J , Ding Y , Wang P , **Wang A** , Xiao D , Xue X , Zhu S , Zhang L , Zhu G. Potential novel immunodominant epitopes derived from MAGE-3 and its significance in serological diagnosis of gastric cancer. J Cancer Res Clin Oncol.2013 July (IF=3.0).

Meeting Presentation:

1. A novel surgical technique as a foundation for in-vivo partial liver engineering in rat. ESSR 2017, 52st Congress of the European Society for Surgical Research, Amsterdam.
2. A novel surgical technique as a foundation for in-vivo partial liver engineering in rat. DTG 2017, 26th Jahrestagung der Deutschen Transplantationsgesellschaft, Bonn.
3. A novel surgical technique as a foundation for in-vivo partial liver engineering in rat. CHFTD 2017, 22th Chirurgischen Forschungstagen, Cologne.
4. A novel surgical technique as a foundation for in-vivo partial liver engineering in rat. Berlin, 2018 DGCH, 135rd Kongresses der Deutschen Gesellschaft für Chirurgie.
5. In-vivo decellularization of liver lobe using single liver lobe perfusion technique. Wilsede 2018, 29th Biotest Wilsede-Workshop.
6. Establishment of in-vivo partial liver decellularization as a foundation for in-vivo liver engineering DTG 2018, 27th Jahrestagung der Deutschen Transplantationsgesellschaft, Berlin.
7. In-vivo decellularization of liver lobe using single liver lobe perfusion technique. CHFTD 2018, 22th Chirurgischen Forschungstagen, Nuremberg.